

***Structural and Electrical studies on ferroelectric
polymer nanocomposites***

A

Thesis

Submitted in the partial fulfilment of requirement for the degree of

MASTER OF TECHNOLOGY

In

MATERIALS AND METALLURGICAL ENGINEERING

By

Richa Sharma

(600902009)

UNDER THE SUPERVISION OF

Dr. K. K. Raina



School of Physics and Material Sciences

Thapar University, Patiala, (Punjab)

June-2011

CERTIFICATE

This is certify that the thesis entitled “**Structural and Electrical studies on ferroelectric polymer nanocomposites**” submitted by **Richa Sharma** in the partial fulfilment of the requirement for the award of degree of **M.Tech in Material Science and Metallurgical Engineering** from the School of Physics and Material Science, Thapar University, Patiala is a record of candidate’s own work carried out by him under my supervision and guidance. The experimental matter embodied in this report has not been submitted in part or full to any other university or institute for the award of any degree.

Supervisor



Dr. K.K. Raina

Deputy Director,

Distinguished Professor,

Thapar University, Patiala

Countersigned by

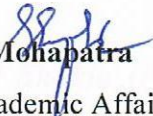


Dr. O.P. Pandey

Professor & Head

Thapar University

Patiala, Punjab



Dr. S.K. Mohapatra

Dean of Academic Affairs

Thapar University,

Patiala, Punjab

ACKNOWLEDGEMENT

*My heartfelt thanks are due to my advisor, **Dr. K. K. Raina, Distinguished Professor and Deputy Director, Thapar University, Patiala** who believes in me and who has guided me to scale heights during my work. Their unique inimitable style has left an indelible impression on me. Their constant encouragement helps and reviews during the course of investigation are invaluable. Nevertheless it helps me acquire and develop some of the skills and intricacies of good independent research. I thank him for his great patience, constructive criticism and myriad useful suggestions apart from invaluable guidance to me.*

*My greatest thanks are to **Dr.O.P. Pandey, Professor & Head, School of Physics and Material Science, Thapar University, Patiala** for his encouragement and execution of thesis work.*

*I am highly grateful to **Dr. Kulvir Singh, Associate Prof., School of Physics And Material Science, Thapar University, Patiala** for their kind help and valuable suggestions and special attention throughout my work.*

*I am also indebted to **Dr. Manoj Sharma, Associate Professor and PG incharge, School of Physics and Materials Science** for their full motivation and appreciation to my work. I am also thankful to all the faculty members of School of Physics and Materials Science, for their constructive suggestions at different stages of my work.*

*It gives me immense pleasure to express my special thanks to **Mr. Ravi Shukla (Ph.D. Scholar)**, who always took keen interest in guiding me during my work. I wish to express my warm and sincere thanks to Research Scholars **Miss Neeraj Sharma, Miss Supreet, Miss Ramnik, Miss Gurpreet** and my colleagues **Vijay Kumar Baliyan, Geetanjali, Vipin Sharma and Meenu** for their support and their timely help and valuable discussions.*

*I owe my sincere thanks to all the staff members of School of Physics and Materials Science for their support and encouragement. Last but not the least; I would like to thank all my **family members and friends** for their moral support that kept my spirit up during the endeavour.*

RICHA SHARMA

ABSTRACT

Nano dispersed (PZT and ZnO) PVDF composite films have been developed via spin coating techniques from the mixed solvent system [mass ratio of 5:5 (THF/DMF)]. The chemical, structural, physical, morphological and dielectric properties were studied by using Fourier transform infrared spectroscopy (FTIR), X-Ray diffraction (XRD), Scanning electron microscopy (SEM) and LCR meter (50Hz to 1 MHz). X-ray diffraction and IR analysis confirmed the formation of pure well crystalline β -phase. SEM studies inferring about the homogenous dispersion of the nano particles in PVDF matrix. Dielectric behaviour of these composite films has been studied to understand the molecular motion at different frequencies. We found the increase in the relative permittivity at the lower concentrations of PZT (.001 wt %) particles, however, in ZnO dispersed composite films permittivity displayed higher magnitude at higher concentration (.007 wt %). The conductivity of such systems has also been estimated. Such composite matrices can be utilized in varying application to fabricate the low and high dielectric constant and memory devices.

CONTENTS

Certificate.....	i
Acknowledgement	ii
Abstract.....	iii
Table of contents.....	iv
List of figures and tables.....	vi
CHAPER 1:	
INTRODUCTION.....	1
1.1 Poly(vinylidene) fluoride(PVDF)	2
1.1.1 Properties and crystal structure of material	2
1.1.2 Phase formation	4
1.1.3 Spherulitic Morphology in PVDF.....	6
1.1.4 Basics of piezoelectricity, pyroelectricity & ferroelectricity in polymers	7
1.1.5 Poling Process	11
1.1.5.1 Electrode Polling.....	11
1.1.5.2 Corona Polling	12
1.2 Zinc oxide (ZnO) Nanoparticle	13
1.3 Lead Zirconate Titanate (PZT).....	13
CHAPER 2:	
LITERATURE REVIEW	14
2.1 Objective of the study	17
CHAPER 3:	
EXPERIMENTAL	18
3.1 Materials.....	18
3.2 Synthesis of β -phase Poly (vinylidene fluoride) (PVDF)	18
3.2.1 Chemical composition	19

3.2.2 Spin coating	19
3.2.3 Cell preparation for dielectric studies	20
3.3 Polymer-Composite preparation	21
3.3.1 Solution processing of ZnO-PVDF nanocomposites	21
3.3.1.1 Chemical composition	21
3.3.2 Solution processing of PZT-PVDF nanocomposites	22
3.3.1.2 Chemical composition	22
3.4 Overview of some important experimental devices	22
3.4.1 Fourier Transformation IR spectroscopy (FTIR)	22
3.4.2 X-ray Diffraction (XRD)	24
3.4.3 Wide Angle X-ray Diffraction	25
3.4.4 Scanning Electron Microscope (SEM)	25
3.4.5 Dielectric measurements	28
CHAPTER 4:	
RESULTS AND DISCUSSION	30
4.1 Chemical Analysis	30
4.2 Structural Analysis	32
4.3 Morphological Analysis	34
4.4 Dielectric spectroscopy	37
4.4.1 Dielectric study of PVDF-PZT composite films	37
4.4.2 Dielectric study of PVDF-ZnO composite films	39
4.5 Conductivity measurement	42
4.4.1 PVDF-PZT composite films	42
4.4.2 PVDF-ZnO composite films	44
Conclusion	46
References	47

LIST OF FIGURES AND TABLES

List of figures

Figure 1.1: Chemical structure of PVDF

Figure 1.2: Atomic structure of PVDF (I) is the β -phase PVDF; (II) is the α -phase PVDF ;(IIp) is of δ -phase PVDF, and (III) is the γ -phase

Figure 1.3: Production and conversion of the crystal forms of PVDF

Figure 1.4: Schematic representation of the structure of polymer spherulitic

Figure 1.5: Tensor directions for defining constitutive relations

Figure 1.6: β -Form PVDF

Figure 1.7: An example of a non-linear polarization response from an applied electric field in a ferroelectric material (hysteresis loop), and a linear polarization of a linear dielectric constant

Figure 1.8: Schematic of the electrode poling system

Figure 1.9: Schematic of the corona poling system

Figure 3.1: Experimental set up for the sample preparation

Figure 3.2: Spin coating unit for depositing thin PVDF composite films

Figure 3.3: Schematic of thin film assembly

Figure 3.4: Prepared cell for dielectric study

Figure 3.5: Solution processing of PVDF nanocomposites

Figure 3.6: Fourier transforms infrared spectrometer

Figure 3.7: X-ray Diffraction

Figure 3.8: Principles of X-ray diffraction spectroscopy

Figure 3.9: Scanning Electron Microscope

Figure 3.10: Working of SEM

Figure 3.11: Interaction of incident beam with sample

Figure 3.12: LCR Meter

Figure 3.13: Optical Microscope and temperature controller

Figure 4.1(a): FTIR spectra of PVDF films cast with mass ratio of 5:5 (THF/DMF): a) as synthesised; b) Annealed at 90°C for 5hrs

Figure 4.1(b): FTIR spectra of PVDF-PZT composite films at different concentration (.001, .003, .005, .007) : a) as synthesized; b) Annealed at 90°C for 5hrs

Figure 4.1 (c): FTIR spectra of PVDF-ZnO composite films at different concentration (.001, .003, .005, .007): a) as synthesized; b) Annealed at 90°C & 150°C for 5hrs.

Figure 4.2 (a): X-ray diffraction pattern of PVDF film (a) without annealing (b) Annealed at 90°C

Figure 4.2(b): X-ray diffraction pattern of PVDF/PZT composite film at varying concentration of PZT (.001, .003, .005, .007wt %) (a) Without annealing (b) Annealed at 90°C for 5hrs

Figure 4.2(c): X-ray diffraction pattern of PVDF/ZnO composite films at varying concentration of ZnO nanoparticle (.001, .003, .005, .007 wt %) (i) Without annealing (ii) Annealed at 90°C for 5hrs.

Figure 4.3 (a): SEM micrograph of pure and PZT dispersed PVDF films at 5000X.

Figure 4.3 (b): SEM micrograph of pure and ZnO nanoparticle dispersed PVDF films at 5000X

Figure 4.4(a): Variation of relative permittivity with frequency at different concentrations of PVDF/PZT at 155°C

Figure 4.4 (b): Variation of dielectric loss with frequency at different concentrations of PVDF/PZT at 155°C

Figure 4.4(c): Variation of relative permittivity with temperature at different concentrations of PVDF/PZT at 100 Hz

Figure 4.4(d): Variation of dielectric loss with temperature at different concentrations of PZT in PVDF at 100 Hz.

Figure 4.4(e): Variation of relative permittivity with frequency at different concentrations of ZnO nanoparticle in PVDF

Figure 4.4(f): Variation of dielectric loss with frequency at different concentrations of ZnO nanoparticle in PVDF at 155°C

Figure 4.4(g): Variation of relative permittivity with temperature at different concentrations of ZnO nanoparticle in PVDF at 100Hz

Figure 4.4 (h): Variation of dielectric loss with temperature at different concentrations of ZnO nanoparticle in PVDF at 100Hz

Figure 4.5 (a): Conductivity measurement of PVDF-PZT system with frequency at 155°C

Figure 4.5 (b): Conductivity measurement of PVDF-PZT system with temperature at 100 Hz

Figure 4.5 (c): Conductivity measurement of PVDF-ZnO system with frequency

Figure 4.5(d): Conductivity measurement of PVDF-ZnO system with temperature

List of tables

Table 1.1: Properties of PVDF

Table 3.1: THF: DMF (5:5)

Table 3.2: Sample1, PVDF-ZnO Composite (.001, .003, .005,.007 wt %)

Table 3.3: Sample2, PVDF-PZT Composite (.001, .003,.005,.007 wt%)

Table4.1: Comparison of relative permittivity of composite films samples at different concentration

Table 4.2: Comparison of conductivity of composite films samples at different concentration

CHAPTER 1

INTRODUCTION

Polymers play an essential and ubiquitous role in everyday life due to their advantages over conventional materials (e.g. metals) such as lightness, resistance to corrosion, low-cost production, and ease of processing. Further improvement of their performance is still being intensely investigated. Altering and enhancement of the polymers properties occur, for example, through doping with various fillers such as metals, semiconductors, organic and inorganic particles and fibres, as well as carbon structures and ceramics[1-4]; thereby enabling polymers to be used as a structural unit . Fillers are used in polymers for a variety of reasons: improved processing, density control, optical effects, thermal conductivity, and control of thermal expansion, electrical properties, magnetic properties, flame resistance, and improved mechanical properties, such as hardness, elasticity, and tear resistance. Polymer composites can be used in many different forms in various areas ranging from structural units in the construction industry to the composites of the aerospace applications.

In the field of polymer science, piezoelectric and ferroelectric polymers play a very important role, as these polymers have applications in the field of microwave modulation, nonlinear optical properties, infrared to visible converter, electromagnetic wave, gas, temperature and pressure sensor [5].

Piezoelectric materials have the ability to transfer energy between the electric and mechanical domains. A lot of attention has been paid to Poly (vinylidene fluoride) PVDF due to its excellent piezoelectric and pyroelectric based properties. Poly (vinylidene fluoride) (PVDF) exhibits higher piezoelectricity than other polymer materials such as nylon and polyvinyl chloride.

Because of its flexibility and easiness to fabricate thin film over an extensive area, PVDF polymer has potential applications in audio and ultrasonic transducers, biomedical sensors, electro mechanical transducers, pyroelectric and optical devices, whilst it has already been applied in the field of hydrophone, medical ultrasonic transducers and robot probe units [6, 7]. The PVDF has been shown to exhibit relatively large elastic modulus. The crystalline β , γ , α and γ phases of PVDF, which carry a permanent polarization, are ferroelectric. This is the basis of a number of technical applications of this material. Polymer nanocomposites are materials in which nanoscopic inorganic particles, typically 10-100 Å in at least one

dimension, are dispersed in an organic polymer matrix. The use of nanoparticles as filler in polymers provides advantages over polymers because they provide improvement in electrical, surface and mechanical properties [8]. These improvements in dielectric properties observed for nano-filled polymer could be due to several reasons. Thus, changes in structural morphology due to incorporation of nanoparticle can influence the dielectric behaviour of nanocomposites [9-10]. Polymer nanocomposites represent a new alternative to conventionally filled polymers. Nanocomposites, so far, have found use in sporting goods, for example athletic shoes and automobile parts like tires, but there is future promise for use in different applications including aerospace. Polyvinylidene fluoride is a semicrystalline polymer that exhibits good mechanical and electrical properties and has excellent polarization stability. So in this study a little attention has been paid to study the nanometric structure of poly (vinylidene fluoride) (PVDF)-zinc oxide (ZnO) nanocomposites and PVDF-Lead zirconate titanate (PZT) nanocomposites.

A dielectric material has an arrangement of electric charge carriers that can be displaced by an electric field. The charges become polarized to compensate for the electric field such that the positive and negative charges move in opposite directions. At the microscopic level, several dielectric mechanisms can contribute to dielectric behaviour. Dipole orientation and ionic conduction interact strongly at microwave frequencies. In general, the dielectric permittivity and the loss factor were found to be higher for nanocomposites than for micro composites at low frequencies. The higher dielectric loss for the nanocomposites was attributed to the enhanced ionic conductivity caused by the contaminants introduced during preparation. Theoretical models have also suggested regarding the influence of interface on nanodielectrics. Tanaka et al. have proposed a multi-core model to understand the dielectric properties of polymer nanocomposites [11].

1.1 Poly (vinylidene fluoride) (PVDF)

1.1.1 Properties and crystal structure of PVDF

Poly (vinylidene fluoride) or **PVDF** ($\text{CH}_2\text{-CF}_2$) is a highly non-reactive and pure thermoplastic fluoropolymer. It is also known as **KYNAR**, **HYLAR** or **SYGEF**. Compared to other fluoropolymers, it has an easier melt process because of its relatively low melting point of around 177°C . It has a low density (1.78) and low cost compared to the other fluoropolymers. It is available as piping products, sheet, tubing, films, plate and an insulator for premium wire. It can be injected, molded or welded and is commonly used in the

chemical, semiconductor, medical and defence industries, as well as in lithium ion batteries. It is also known as poly (1, 1-difluoroethylene) with a repeat unit ($\text{CH}_2\text{-CF}_2$) as shown in fig (1.1). Poly (vinylidene Fluoride (PVDF) was polymerized for the first time in the 1940s. In 1969, Kawai found that PVDF exhibited an unusually large piezoelectric effect after poling [12], the process in which a high electric field will be applied. In early 1970s, it was discovered that PVDF is a ferroelectric material. PVDF and its copolymers have been widely studied because of their interesting piezoelectric, pyroelectric, and dielectric properties. In dielectric studies [13-14], PVDF has a very high dielectric permittivity among polymer materials and high dc dielectric strength, which make PVDF a very promising dielectric material for use in energy storage capacitors. Polyvinylidene Fluoride has a simple chemical structure (shown in fig.1.1) [15]. Table 1.1 shows the some important properties of PVDF.

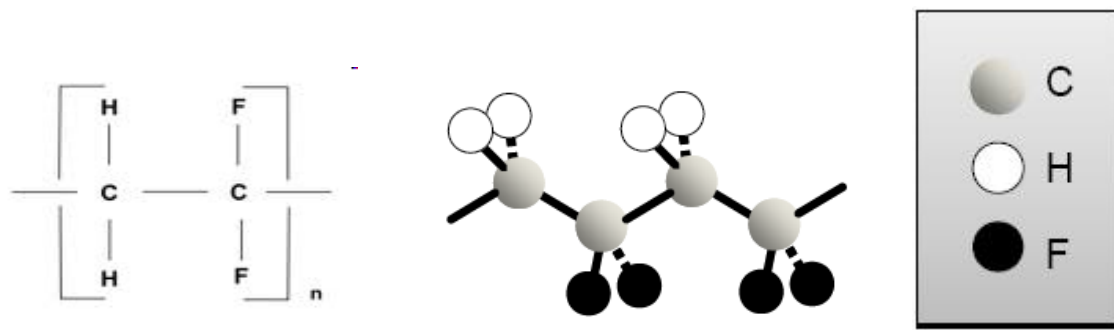


Fig.1.1 Chemical structure of PVDF

Table 1.1 Properties of PVDF [16]

Property	PVDF
Density (10^3 kg m^{-3})	1.78
Acoustic velocity (km s^{-1})	2.26
Acoustic impedance (MRayl)	20
Elastic constant, C (10^9 N m^{-2})	9.10
Coupling factor, k_t	0.20
Piezoelectric constants	
e_{33} (C m^{-2})	-0.16
h_{33} (10^9 V m^{-1})	-2.90
g_{33} (Vm N)	-0.32
d_{33} (pC N^{-1})	25.00
Dielectric constant, ϵ_s/ϵ_0	6.20
Mechanical Q factor	5-10
Mechanical loss tangent, $\tan \delta_m$	0.10
Dielectric loss tangent, $\tan \delta_e$	0.25
Pyroelectric constant ($\mu\text{C m}^{-2} \text{ K}$)	35.00
Coercive field, E_c (MV m^{-1})	45.00
Thermal stability ($^\circ\text{C}$)	90.00
Transmitting efficiency, Y_T	6.9
Receiving efficiency, Y_R	1.35
$Y (= Y_T Y_R)$	9.30

1.1.2 Phase formation

PVDF is a semi crystalline polymer with a crystalline fraction of about 50 to 60% depending on the amount of chain ordering defects. Crystallinity in polymers means that the chains are packed together more efficiently and tightly which increases the density of the polymer, as well as leads to an increase in the mechanical properties of the polymers. PVDF exists in several forms: α (TGTG'), β (TTTT), γ (TTTGT'TTG') and δ - phases, depending on the chain conformations as trans (T) or gauche (G) linkages, among which the β phase has gained substantial importance due to its advantageous pyro- and piezoelectric properties.

The first one is the β -phase(fig.(1.2I)) forms from α -phase, and is the most stable phase by different methods are shown in figure (1.3). Mechanical stretching to about 300% of its original length at a temperature around 100°C, then by poling at high electric field which is the most known method, followed, or annealing at high temperature or very high pressure, or by drawing at low temperature, and ultra-drawing at high temperature. The β -phase forms from δ -phase by poling at high electric field. There are some possibilities to have β -phase from γ -phase by drawing and annealing at very high temperature.

The second one is α -phase which is the most stable phase at room temperature (fig.(1.2II)); therefore PVDF films crystallize into this phase from the melt at all temperatures as seen in figure (1.3).[17-18]

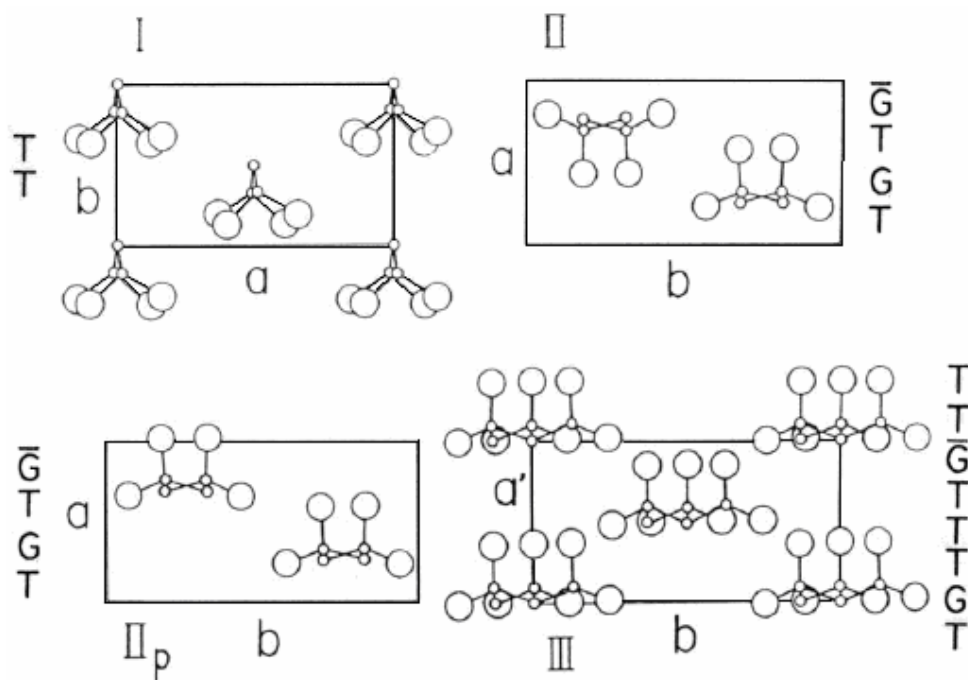


Figure 1.2: Atomic structure of PVDF (I) is the β -phase PVDF; (II) is the α -phase PVDF ;(IIp) is of δ -phase PVDF, and (III) is the γ -phase

The third phase is called polar δ -phase as shown in figure (1.2IIp), which can be transformed from α -phase by applying an electric field greater than, or equal to 130 MV/m. Thus producing an inversion of the dipole moments in alternated chains. It has an orthorhombic lattice. The unit cell dimensions and the configuration are the same as the α -phase.

The fourth phase is called γ -phase shown in figure (1.2III) has a trans-trans-trans-gauche (TTTG) conformation; the molecular chains are packed in a parallel non-Centro symmetric, polar crystal. Figure (1.3) shows that the γ -phase is obtained by annealing α -phase at high temperature, or annealing at high pressure [19]. Annealing δ -phase at high temperature also forms γ -phase.

Because of the strong electro negativity of fluorine atoms compared to those of hydrogen and carbon, each PVDF chain possesses a dipole moment perpendicular to the polymer chain.

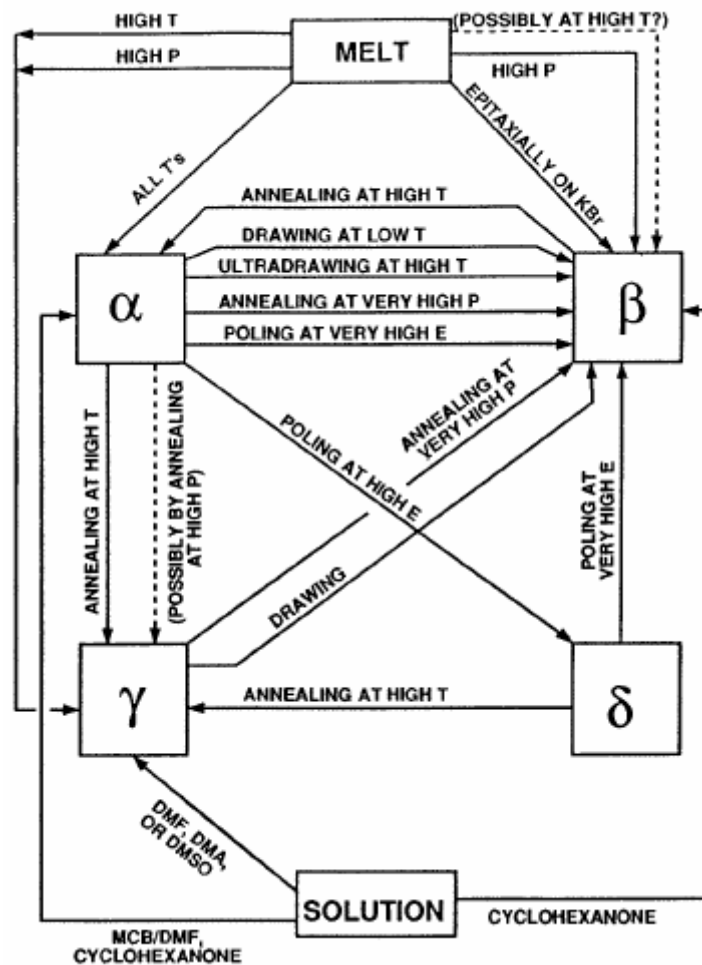


Figure 1.3: Production and conversion of the crystal forms of PVDF

1.1.3 Spherulitic Morphology in PVDF

The most interesting of the semicrystalline polymers are PVDF, polyvinyl fluoride (PVF) and related copolymers. These polymers crystallize much like polyethylene because the fluorines, unlike larger chlorines, are close enough in size to hydrogen so as not to interfere with regular packing.

PVDF crystallizes from the melt into spherulitic structures. Spherulites are composed of highly ordered lamellae, which result in higher density, hardness. These lamellae are typically 10-20 nm thick, depending on crystallization conditions [20]. A schematic diagram of a spherulite within an unoriented semicrystalline polymer is shown in fig. (1.4).

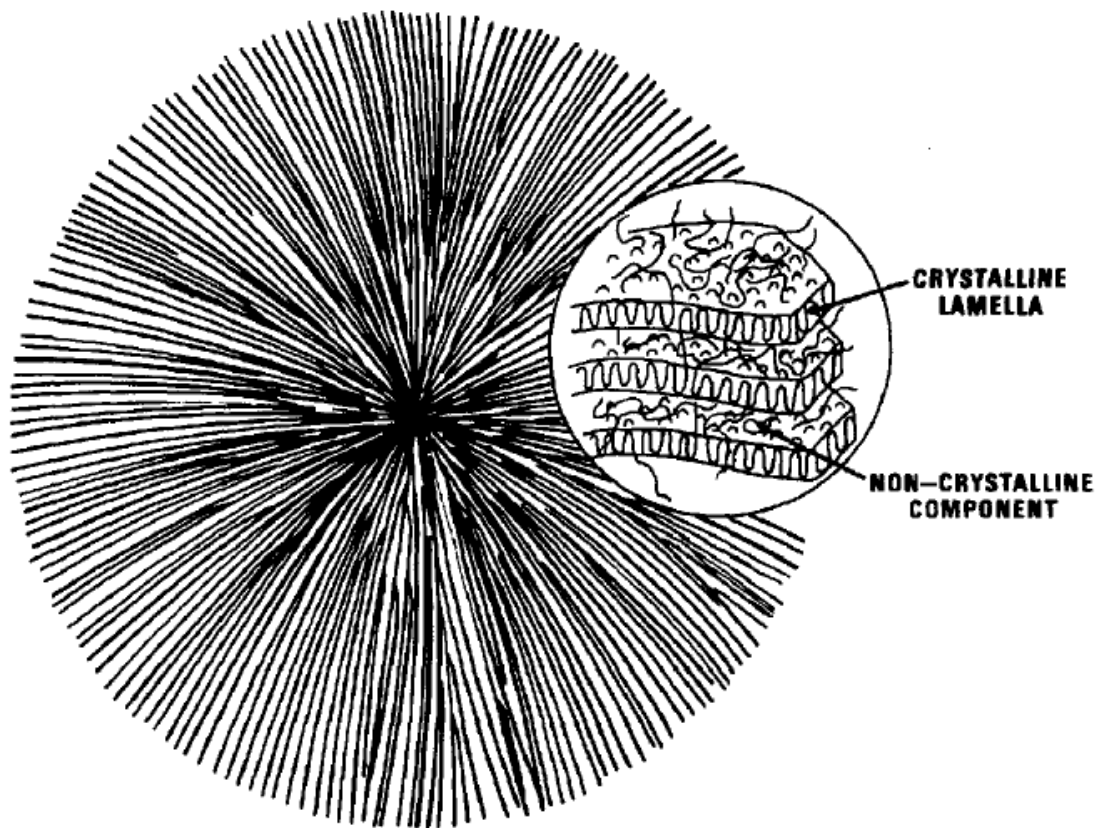


Figure 1.4: Schematic representation of the structure of polymer spherulitic

Figure (1.4) illustrates the essential features of spherulitic morphology in semicrystalline polymers such as PVF and PVDF. Molecular chain axes are approximately normal to the surface of lamellar platelets which grow radially from the centre of the structure.

Annealing or crystallizing for longer times, at higher temperatures and pressures increases the lamellar thickness and perfection which results in a higher sample density. The crystals grow

in the form of spherulites and studies of the morphology of PVDF show that three crystal phases have distinct morphology and can grow simultaneously from the melt or one phase can grow at the expense of another. The polymers currently of greatest interest for piezoelectric applications, PVF and PVDF, are of the order of 50-70% crystalline. The amorphous phase is probably mostly confined to layers between the crystal lamellae. The amorphous phase seems to have normal super cooled liquid properties with a liquid-glass transition region around - 50 °C.

1.1.4 Basics of piezoelectricity, pyroelectricity & ferroelectricity in PVDF

Both piezoelectricity and pyroelectricity were observed over 30 years ago in PVDF. Piezoelectric transducers made by solvent casting were soon commercially available, though it took a decade to establish that ferroelectricity was the origin of these effects in PVDF.

- **Piezoelectricity in PVDF**

The phenomenon of piezoelectricity was first discovered just over a century ago by the Curie brothers, Pierre and Jaques. Piezoelectricity is the ability of a material to convert mechanical stimulus to electrical response, and vice versa. A mechanical stress applied to a piezoelectric will produce an electric potential across its boundaries. Likewise an electric potential created across a piezoelectric's boundaries will result in a mechanical deformation of the material [21]. Many other materials exhibit the piezoelectric effect, including quartz analogue crystals like berlinite (AlPO_4) and gallium orthophosphate (GaPO_4), ceramics with perovskite or tungsten-bronze structures (BaTiO_3 , SrTiO_3 , PbZrTiO_3 , KNbO_3 , LiNbO_3 , LiTaO_3 , BiFeO_3 , Na_xWO_3 , $\text{Ba}_2\text{NaNb}_5\text{O}_{15}$, $\text{Pb}_2\text{KNb}_5\text{O}_{15}$) . Polymeric materials like rubber, wool, hair, wood fiber, and silk exhibit piezoelectricity to some extent. The polymer polyvinylidene fluoride, PVDF, exhibits piezoelectricity several times larger than quartz. Polarization is defined as the separation of the center of the positive and negative electric charges, making one side of the crystal positive and the opposite side negative. The electrical response of piezo-materials is a function of both stress (T) applied to the electrode area and the mechanical strain (S) that the material experiences [22] .The constitutive relations of piezoelectricity in materials can be derived using a tensor notation. The directions are depicted in the figure (1.5) below.

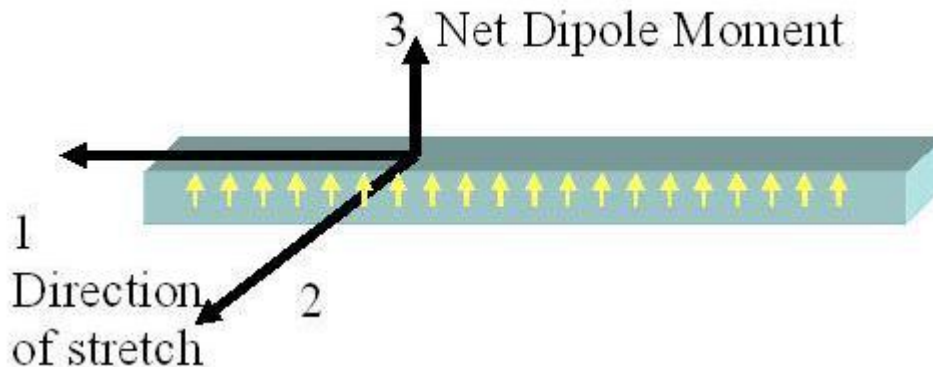


Figure 1.5: Tensor directions for defining constitutive relations

PVDF is a piezoelectric material. PVDF exhibits permanent polarization by a procedure called poling, i.e. by being subjected to high DC electric field at elevated temperature. That means it change its shape when placed in electric field. Because fluorine is so much more electronegative than carbon, the fluorine atoms will pull electrons away from the carbon atoms to which they are attached. This means the $-CF_2-$ groups in the chain will be very polar, with a partial negative charge on the fluorine atoms and a partial positive charge on the carbon atoms. So when they're placed in an electrical field, they align. This causes the polymer sample to deform, all those $-CF_2-$ groups trying to align. PVDF is known to possess especially strong piezoelectric coupling among polymeric materials. So the source of PVDF's piezoelectricity is a dipole created by Fluorine and Carbon bonded in its structure. The dipole is strongest when PVDF is in its β -form structure (Figure 1.6). This structure aligns all of dipoles throughout the polymer chain creating polarization that extends to the boundaries of the PVDF. These dipoles are key to allowing PVDF to act as a sensor. Mechanical expansion/compression of the dipoles creates a charge distribution that produces a subsequent potential difference across PVDF [23].

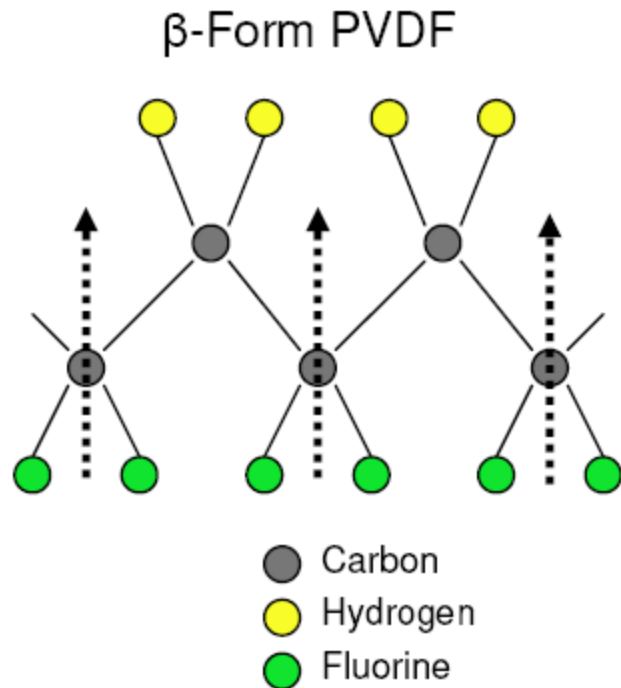


Figure 1.6: β -Form PVDF

- **Pyroelectricity in PVDF and temperature effect**

PVDF is also pyroelectric, producing electrical charge in response to a change in temperature. Pyroelectric sensor materials are usually dielectric materials with a temperature-dependent dipole moment. As these materials absorb thermal energy, they expand or contract, which leads to secondary piezoelectric signals. The output current is proportional to the rate of temperature change ΔT . The amount of electrical charge produced per degree of temperature increase (or decrease) is described by the pyroelectric coefficient ρ . The voltage V produced in a given film of permittivity ϵ , and thickness t is given by the following equation.

$$V = \rho \cdot t \cdot \Delta T / \epsilon$$

- **Ferroelectricity of PVDF**

PVDF is the most widely used ferroelectric polymer and is manufactured in large quantities for a wide variety of applications, ranging from protective coatings to ultrasound transducers.

Ferroelectric materials are classified as nonlinear dielectrics. This means that when an electric field (E) is applied to the material, the stored charge (Q) does not result in a linear response.

Though PVDF shows clear repeatable polarization hysteresis, there was doubt initially that this was of ferroelectric origin because many polymers exhibit long-lived but transient hysteresis due to either charge injection or induced polarization.

Figure 1.7 shows an example of this effect with a plot showing a linear and nonlinear response. The nonlinear response for ferroelectric materials is called a hysteresis loop. At lower applied fields, the polarization is similar to a linear dielectric and is fully reversible. As the applied field increases to a saturation point (P_{sat}), polarization will remain after the electric field is removed. Polarization saturation (P_{sat}) is the point at which polarization will no longer increase with increasing electric field. The remaining polarization in the dielectric material after the field has been removed is called the remanent polarization (P_r). Remanent polarization is basically a measure of the residual alignment in the domains due to the applied field. The coercive field (E_c) is the amount of applied electric field needed to return the material to a state of zero polarization. Several factors including composition, thickness, and electrode properties affect the shape and the values of the hysteresis loop. Each of these can have a large influence on the ferroelectric and piezoelectric properties of the resulting material. In PVDF the polarization reversal is likely connected to change in conformation of molecular chain between the phases at high temperature.

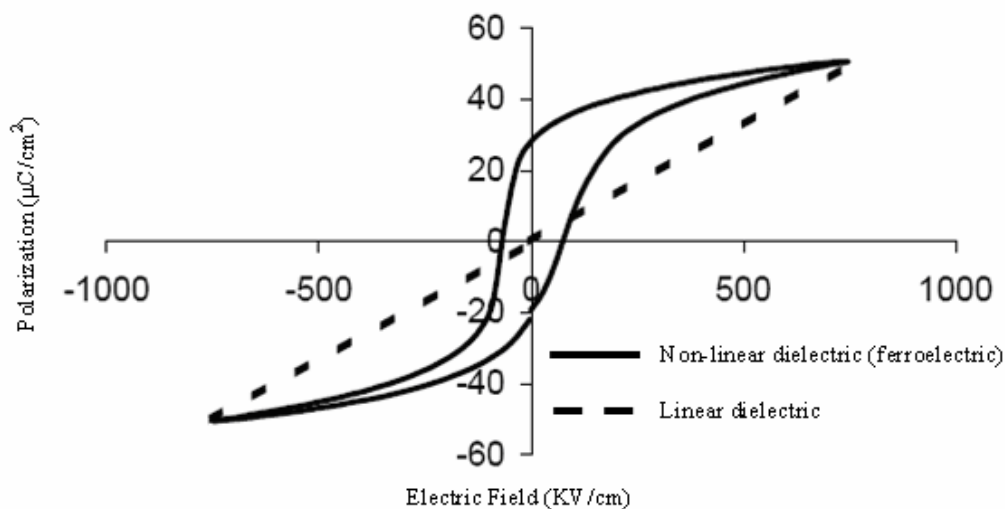


Figure 1.7. An example of a non-linear polarization response from an applied electric field in a ferroelectric material (hysteresis loop), and a linear polarization of a linear dielectric constant.

1.1.5 POLING PROCESS

Generally speaking in order to obtain β -PVDF film it is necessary to stretch the inactive α -PVDF film up to four times of its original length, then expose the sample to a very high electric field at elevated temperature, and finally the temperature is then lowered in the presence of the electric field so that the domains are locked in the polarized state. The second step is called “poling process”. After the poling process, the random dipolar moments tend to align along the direction of the external longitudinal electric field. The stretching process alone does not induce a complete α to β transformation.

While the theoretical results of molecular dynamics (MD) carried out by Ramos et al. suggest that this transformation can also be achieved without mechanical stretching, when a sufficiently strong electric field (e.g., 100 MV/m) is applied [25]. Perlman et al. also found that the piezoelectric and pyroelectric constant of PVDF films and copolymers can be increased by nearly 200% when they are simultaneously subjected to stretching and poling process [26]. Poling processes in PVDF are still quite empirical because a thorough understanding of the physical processes involved in poling has not been fully established. There are typically two common techniques for polarization induction of PVDF films: **electrode and corona poling**.

1.1.5.1 Electrode Poling

Figure (1.8) shows the schematic diagram of the electrode poling system [27]. The conducting electrodes (top and bottom), which are either evaporated, sputtered, or painted on the PVDF film surfaces, are required for poling process.

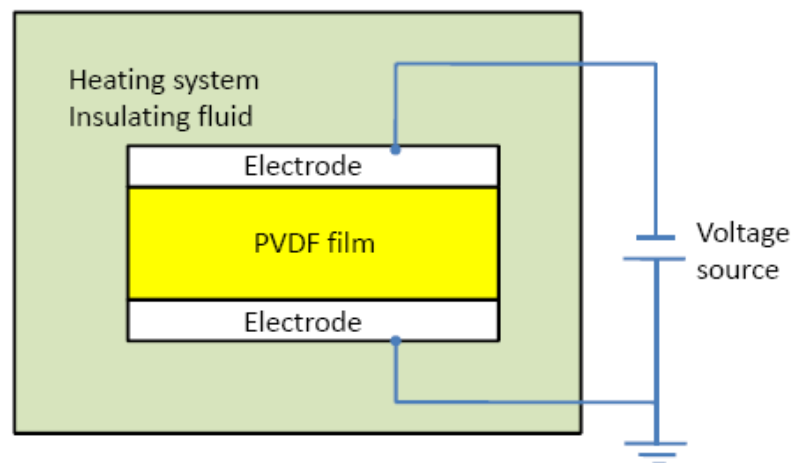


Figure1.8: Schematic of the electrode poling system.

When the voltage potential is applied to the electrodes then an electric field is produced across the sample. The poling can be done in air without arcing provided that the electrodes do not reach the edge of the film. Otherwise the PVDF film might need to be placed in a vacuum or submerged in an insulating fluid, which can prevent arcing that will damage the material. Either static or sinusoidal electric fields at low frequency (MHz) can be applied to the sample during electrode poling. A constant electric field is held on the sample from 10-30 minutes up to 2 hours. A variable field could reduce the probability of dielectric breakdown caused by high voltages for a prolonged period of time.

1.1.5.2 Corona Poling

The schematic diagram of **corona poling** is shown in Figure (1.9). In corona poling the bottom surface with electrode is placed on a heating plate and connected to the ground. A corona tip is suspended above the sample and is applied to high (8-10 kV) voltages. The grid is usually placed at the distance of 3-4 mm from the sample to control the magnitude of the applied electric field.

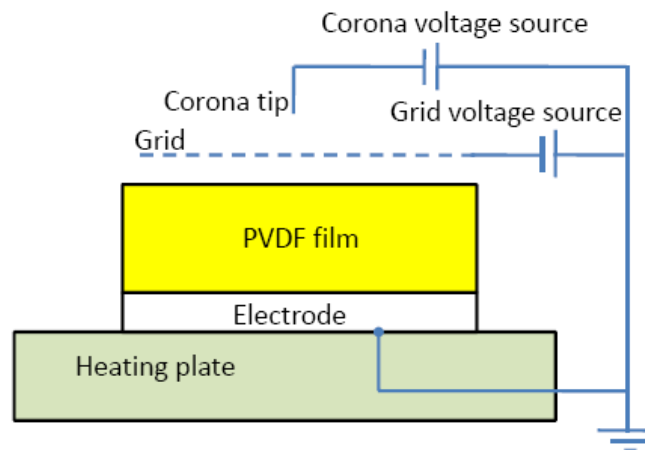


Figure 1.9: Schematic of the corona poling system

When the corona discharge is triggered, the ionized particles are accelerated towards the ground and deposited on top surface of the sample, which forms the poling electric field between the top surface and the ground. Corona poling is useful for large area poling and essentially it generates electrodes during the poling. The magnitude of the electric field and sample temperature are the key for the poling process. The higher the applied electric field, the higher the induced polarization provided that the poling field is larger than the coercive field of PVDF.

1.2 Zinc oxide (ZnO) Nanoparticle

Nanometric metals and inorganic oxides are added to the polymer matrix to improve the mechanical, tribological, and electrical properties of polymer. Semiconductor nanoparticles are a very important topic in the ongoing research activity across the world. As the semiconductor particles exhibit size-dependant properties like scaling of the energy gap and corresponding change in the optical properties, they are considered as the front runners in the technologically important materials. Zinc oxide is a wurtzite type semiconductor material. Zinc oxide is attracting tremendous attention due to its interesting properties like wide direct band gap of 3.3 eV at room temperature and high exciton binding energy of 60 meV. Recently, special attention has been devoted to the morphology, as ZnO can form different nanostructures [28-30]. Thermal stability, irradiation resistance and flexibility to form different nanostructures are the advantages that expedite its potential wide applications in photo detectors , surface acoustic wave devices , ultravioletnanolaser , varistors , solar cells , gas sensors , biosensors , ceramics , field emission , and nanogenerator .

1.3 Lead Zirconate Titanate (PZT)

Lead zirconate titanate ($\text{Pb}[\text{Zr}_x\text{Ti}_{1-x}]\text{O}_3$ $0 \leq x \leq 1$), also called PZT is a ceramic pervoskite material that shows a marked piezoelectric effect. PZT-based compounds are composed of the chemical elements lead and zirconium and the chemical compound titanate which are combined under extremely high temperatures. Being pyroelectric, this material develops a voltage difference across two of its faces when it experiences a temperature change. As a result, it can be used as a sensor for detecting heat.

It is also ferroelectric, which means it has a spontaneous electric polarization (electric dipole) which can be reversed in the presence of an electric field.

Over the past few decades, there has been significant growth in the development and application of piezoceramic polymer composites. This growth is due to their use of complementary elements, which combine the high electromechanical coupling of piezoelectric materials with the high dielectric strength of the polymer matrix.

CHAPTER 2

LITERATURE REVIEW

PVDF is polymorphic and can crystallize in 5 different forms. Lovinger [31] reviewed the various polymorphic structures and properties of PVDF. The major crystal forms of PVDF involve different chain conformations each of which possesses a component of a net dipole moment perpendicular to the chain.

The polymer chains of PVDF pack the unit cell in two different ways. Either they are additive and the crystal possesses a net dipole or they pack with dipoles in opposite directions so there is no net dipole in the crystal. The polar conformations are piezoelectric while the antipolar ones are not. Commercial polymerization under standard conditions usually generates alpha phase of PVDF. This is an antiparallel array and there is no net dipole in the crystal [32].

The beta phase of PVDF has a net dipole moment and the best piezoelectric coefficient after the poling process. Hence β phase is the most important in terms applications and a lot of research is being done on it. The β phase has all-trans although successive $-\text{CF}_2$ groups must be deflected by 7° in opposite directions from planar zig-zag conformation to accommodate the fluorine atoms [33].

β -phase can also be induced by using different kind of solvents. There is a strong effect of solvent molecules with poly (vinylidene fluoride) (PVDF) chains on the structure and crystallization behaviour of PVDF in films obtained by solution casting. In a single solvent system, the film cast from the good solvent of N,N-dimethylformamide (DMF), showed dominantly β -phase crystals with the highest PVDF crystallinity (50.6%) and the largest spherulite size, about 4 mm, at the top surface. The samples deposited from good swelling agents, such as tetrahydrofuran (THF) and methyl ethyl ketone (MEK), exhibited mainly the original α -phase with some amount of β -phase crystals; the crystallization behaviour and the morphology of the surface were similar to the original PVDF resin, because of the only partially dissolved PVDF chains in these two solvents. In a mixed solvent system (THF/DMF), the β - phase formation with linearly increment in the DMF content resulted in the clear spherulitic structure with higher percentage of β -phase. Surface of the film deposited by such mixed solvent systems consisted of β - spherulites with average size of about 3 mm, which were smaller than those grown from pure DMF, because of the increased crystallization rate in the mixed solvent[34]

In 1969, Kawai [35] discovered that a strong piezoelectric effect could be induced in Polyvinylidene Fluoride (PVDF) by applying an electric field. He showed that poled thin films exhibited a large piezoelectric coefficient.

In 1971, Bergman et al. [36] and Wada et al. [37] discovered that PVDF films polarized this way also exhibited pyroelectricity with pyroelectric figures of merit comparable to crystalline pyroelectric detectors.

In 1989, Barsky et al. [38] developed a PVDF sensor-based feedback manipulating microgripper system.

Niu et al. [39] revealed a method for the preparation of mechanically strong yet electrically conductive polyvinylidene fluoride, (PVDF)-CNT composite by two different methods. In solution method, PVDF was first dissolved in a solvent such as acetone; CNTs were then added into the solution and sonicated. The composite was then precipitated with a precipitating component such as water, filtered and dried. In melt compounding method, PVDF was mixed with CNTs in a mixer at high temperatures to melt and compound PVDF into CNTs to form the composite. They found that the composite prepared by the solution method were better electrical conductors than that by the melt compounding method. They claimed that this composite had a higher level of conductivity than other known polymer composites.

Shukla et al.[40] concluded a new approach inducing structural phase transition from pristine α -crystal phase of PVDF to β -crystal phase has been attempted via nanocomposites formation of PVDF using nanoclay. XRD and FTIR data confirmed phase transition in PVDF. However a complete phase conversion could not be achieved and the composite film comprises of both α and β -phases with enhanced β phase fraction controlled by clay concentration. The enhancement in β -phase has been reflected in terms of improved dipolar ordering in composite films when compared with pure PVDF. This has been indicated in the results of dielectric properties observed as a function of temperature as well as piezoelectric coefficient measurement.

Yi and Liang [41] revealed the mathematical modeling, analysis, and experiments of a new deformation and motion measurement sensor that is made of polyvinylidene fluoride (PVDF) thin-film. The PVDF-based deformation sensor is designed and fabricated for several applications, such as deformation detection of automotive tires and insect locomotion measurements.

D.R. Dillon et al. [42] produced Polyvinylidene fluoride (PVDF)–nanoclay nanocomposites by both solution casting and co-precipitation methods with the nanoclay loading of 1–6 wt%.

β - form PVDF was observed in all the nanocomposites regardless of the nanoclay morphology and contents. Both crystallization and melting temperatures of PVDF were increased with the addition of nanoclay, possibly due to the formation of the β -form PVDF.

M. S. Gaur, A. P. Indolia [43] studied in detail about the thermally stimulated dielectric properties of polyvinylidene fluoride–zinc oxide nanocomposites. They prepared a Thirty micrometer thick polyvinylidene fluoride (PVDF)–zinc oxide (ZnO) nanocomposite samples in the mass ratio of ZnO (1–6% (w/w)) by solution mixing method. The SEM and AFM images show the presence of different components such as nanoparticles, amorphous and crystalline phases in nanocomposite samples. Dielectric properties of polymer nanocomposite based on PVDF and ZnO of different mass/% compositions have been studied to understand the molecular motion at different frequencies in the temperature range from 300 to 500 K. The permittivity of the nanocomposites decreases with frequency, while increases with the increasing temperature and ZnO content. The loss peak that disappeared at higher frequency is the remarkable result of this study.

In recent years, composites composed of electro - ceramics and ferroelectric polymer are very attractive for applications since they exhibit high piezoelectric and pyroelectric properties, low acoustic impedance matching with water, and furthermore, their properties can be tailored to various requirements. Zhang De-Qing et al.[44] Structural and Electrical Properties of PZT/PVDF Piezoelectric nanocomposites prepared by Cold-Press and Hot-Press Routes. H Tang et al [45] investigated the role of filler aspect ratio in nanocomposites for energy storage. They synthesized the nanocomposites using lead zirconate titanate (PZT) with two different aspect ratio (nanowires, nanorods) dispersed its various volume fraction into polyvinylidene fluoride (PVDF) matrix. Dielectric spectroscopy measurements on the composites showed that the nanocomposites with PZT NWs have a higher dielectric permittivity and lower loss tangent than composites with lower aspect ratio fillers. The energy density of nanocomposites increased with the volume fraction of PZT filler.

2.1 OBJECTIVE OF THE STUDY

Poly (vinylidene fluoride) (PVDF) is the only commercially available piezoelectric polymer. It is also a pyroelectric polymer. PVDF has interesting mechanical and electrical properties, which make it an attractive candidate for several applications in the aerospace industry. PVDF has four known crystal morphologies, and has the highest piezoelectric coefficients among synthetic polymers. The literature review gives an idea that the physical properties of polymer can be enhanced by mean of adding nanoparticles, carbon nanotubes and clay where the concentration can be varied and optimize to understand the physical structural and chemical properties of the composite system. Over the past few decades, there has been significant growth in the development and application of piezoceramic polymer composites. This growth is due to their use of complementary elements, which combine the high electromechanical coupling of piezoelectric materials with the high dielectric strength of the polymer matrix.

In this work, zinc oxide (ZnO) nanoparticle and Lead zirconate titanate (PZT) with different weight fractions are dispersed in poly (vinylidene fluoride) matrix to make composite. A uniform distribution of nano particles within a polymer matrix is necessary conditions for the effective improvement of the properties of the composites. The study will be focused on the examination of the structural, chemical and dielectric properties of polymer composites.

The main objectives of study are:

- 1) Synthesis of β -phase in poly (vinylidene fluoride) PVDF polymer
- 3) Synthesis of nano based polymer composite.
- 4) Characterization of nano composite by using various techniques.

3.1 Materials

The materials used in this study were poly (vinylidene) fluoride PVDF (pellet) typical $M_w = 530,000$ (Aldrich), Zinc oxide (ZnO) nanopowder having particles size around 7 nm, Lead zirconate titanate (PZT) powder with particle size 137 nm. The solvents used during synthesis were tetrahydrofuran (THF), C_4H_8O ($M_w = 72.11$, stabilized) (s.d.fine-chem Ltd) and N, N-Dimethylformamide DMF, C_3H_7NO ($M_w = 73.09$) (s.d.fine-chem Ltd). All the materials used as received without any further purification.

3.2 Synthesis of β -phase Poly (vinylidene fluoride) (PVDF)

The glass wares (three necks round bottom flask, measuring cylinder, and beaker) were first cleaned and rinsed with distilled water and then dried. All the materials and solvents are weighed with help of electronic weighing balance and mixed in cleaned round bottom flask. A 100 ml three neck flasks is charged with poly (vinylidene fluoride) dissolved in THF/DMF mixture with 5:5 mass ratio. The reactants were refluxed at $60^\circ C$ with gentle stirring for 3h on hot plate (fig. 3.1).

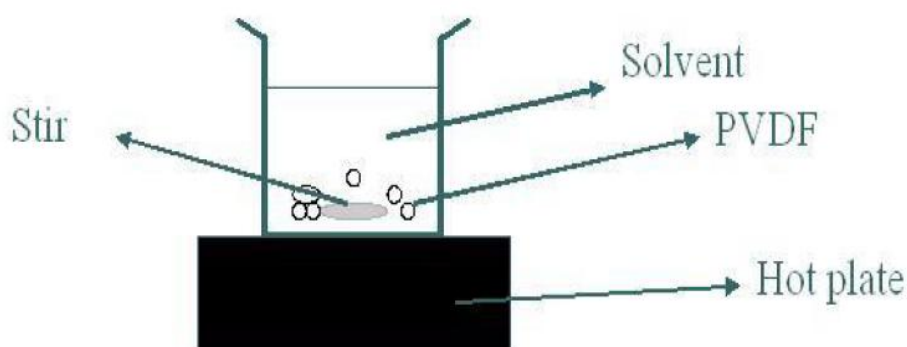


Figure 3.1: Experimental set up for the sample preparation

After stirring for 3h, reaction mixture is allowed to cool to room temperature. The transparent solution is cast on glass substrates by spin coating. The residue of THF and DMF was allowed to evaporate in air for about one week at room temperature. Free standing thin films (thickness $\sim 5-7 \mu m$) on glass substrate were formed at the end with the complete evaporation of solvents.

3.2.1 Chemical composition

Table 3.1 THF: DMF (5:5)

Sr. No.	Chemical name	Chemical formula	Quantity of material used
1.	Poly(vinylidene fluoride) (PVDF)	$-(\text{CH}_2\text{-CF}_2)-$	1g
2.	Tetrahydrofurane (THF)	$\text{C}_4\text{H}_8\text{O}$	5 ml
3.	N, N-Dimethylformamide (DMF)	$\text{C}_3\text{H}_7\text{NO}$	5 ml

3.2.2 Spin coating

Spin coating is the preferred method for deposition of uniform thin films on flat substrates. In the typical procedure the appropriate amount of polymer solution is poured in the center of the substrate.



Figure 3.2: Spin coating unit for depositing thin PVDF composite films

The substrate is then rotated at high speed in order to spread the fluid by centrifugal force. Rotation is continued for some time, with fluid being spun off the edges of the substrate, until the desired film thickness is achieved. The applied solvent is usually volatile, providing for

its simultaneous evaporation with the passage of time. Higher the angular speed of spinning, the thinner the film. The thickness of the film also depends on the concentration of the solution and the solvent

3.2.3 Cell preparation for dielectric studies

Dielectric studies of thin film samples were carried out by depositing thin film on ITO coated glass substrate in spin coating unit and sandwiches by another ITO coated glass plate followed by sealing and electrical connection. To make cell schematic of thin film assembly shown in figure 3.3.

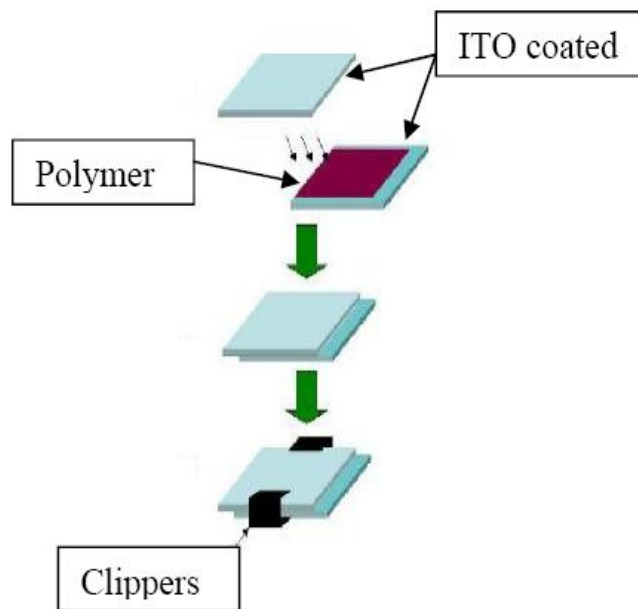


Figure 3.3: Schematic of thin film assembly

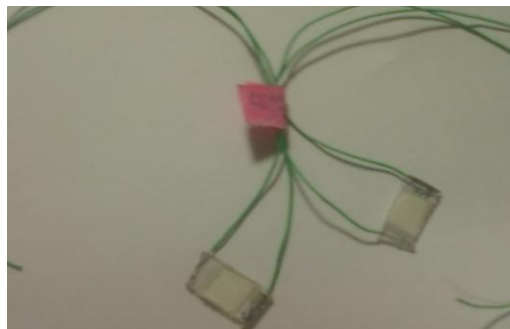


Figure 3.4: Prepared cell for dielectric study

3.3 Polymer-Composite preparation

3.3.1 Solution processing of ZnO-PVDF nanocomposites

To prepare composite system the first step was same as the synthesis of PVDF samples. In Second step, an appropriate amount of ZnO-nanoparticle was added to mixture of (PVDF) poly (vinylidene) fluoride, an organic solvent N, N dimethylformamide (DMF) and tetrahydrofuran (THF). The final mixture was gently refluxed at 60°C for 3h. After stirring, the solution was sonicated for 2h.



Figure 3.5: Solution processing of PVDF nanocomposites

The ZnO nanoparticles-PVDF nanocomposites were prepared with different concentrations of ZnO-nanoparticles in PVDF. This final mixture is further treated for making composite film by using Spin Coating. The residue of DMF and THF was allowed to evaporate in an air oven for about week at room temperature. Free-standing films (thickness ~ 4-6 μm) on glass substrate were formed at the end when the solvent completely evaporated.

3.3.1.1 Chemical composition

Table3.2: Sample1, PVDF-ZnO Composite (.001, .003, .005, .007 wt %)

Sr. No.	Chemical name	Chemical formula	Quantity of material taken
1.	Poly(vinylidene fluoride)(PVDF)	-(CH ₂ -CH ₂)-	1 g
2.	Zinc oxide nanoparticle	ZnO	0.001,0.003,0.005,0.007g
3.	Tetrahydrofuran(THF)	C ₄ H ₈ O	5ml
4.	N,N-Dimethylformamide(DMF)	C ₃ H ₇ NO	5ml

3.3.2 Solution processing of lead zirconate titanate (PZT) -PVDF composite

An appropriate amount of PZT was added to mixture of PVDF poly (vinylidene) fluoride, an organic solvent (DMF) N, N dimethylformamide and (THF) tetrahydrofuran. The final mixture was then thoroughly mixed by magnetic stirrer at 60°C for 3h. After stirring, the solution was sonicated for 2h. The PZT -PVDF samples were prepared with different concentration of PZT. This final mixture is further treated for making of thin film and bulk films by using various techniques i.e. spin coating and solution cast method. The residue of DMF and THF was allowed to evaporate in an air oven for about one week at room temperature. Free-standing films (thickness ~ 4-6 μm) on glass substrate were formed in the end when the solvent completely evaporated.

3.3.2.1 Chemical composition

Table3.3: Sample2, PVDF-PZT Composite (.001, .003, .005, .007 wt %)

Sr. No.	Chemical name	Chemical formula	Quantity of material taken
1.	Poly(vinylidene fluoride)(PVDF)	$-(\text{CH}_2-\text{CH}_2)-$	1 g
2.	Lead zirconate titanate(PZT)	PZT	0.001,0.003,0.005,0.007g
3.	Tetrahydrofuran(THF)	$\text{C}_4\text{H}_8\text{O}$	5ml
4.	N,N-Dimethylformamide(DMF)	$\text{C}_3\text{H}_7\text{NO}$	5ml

3.4 Overview of some important experimental devices

3.4.1 Fourier transformation IR spectroscopy (FTIR)

Fourier Transform Infrared Spectroscopy (FTIR) is based on the fundamental principles of molecular spectroscopy. Fourier Transform Infrared Spectroscopy (FTIR) provides specific information about chemical bonding and molecular structures, making it useful for analyzing organic materials and certain inorganic materials. The basic principle behind molecular spectroscopy is that specific molecules absorb light energy at specific wavelengths, known as their resonance frequencies. For example, the water molecule resonates around the 3450 wave number in the infrared region of the electromagnetic spectrum. An FTIR spectrometer works by taking a small quantity of sample and introducing it to the infrared cell. Some of the infrared radiation is absorbed by the sample and some of it is passed through (transmitted).

The resulting spectrum represents the molecular absorption and transmission, gives information of type of bonding in the sample. This makes infrared spectroscopy useful for several types of analysis. Experimental set up is shown in figure 3.6 below.



Figure 3.6: Fourier transforms infrared spectrometer

The original infrared instruments were of the dispersive type. These instruments separated the individual frequencies of energy emitted from the infrared source. This was accomplished by the use of a prism or grating. A grating is a more modern dispersive element which better separates the frequencies of infrared energy. The detector measures the amount of energy at each frequency which has passed through the sample. This results in a spectrum which is a plot of intensity vs frequency. Fourier Transform Infrared (FT-IR) spectrometry was developed in order to overcome the limitations encountered with dispersive instruments. The main difficulty was the slow scanning process.

So, Why an FT-IR Spectrometer?

Choose an FT-IR over a dispersive instrument if:

- You work in the infrared
- You need high spectral resolution
- You work with weak signals

- You need to acquire your spectra quickly and with high S/N ratio
- You need high spectral accuracy

FT-IRs possess strong theoretical reasons that enable them to excel in these categories. How much of this potential advantage is realized in your application depends strongly on the instrument's design and the particulars of your measurement.

What information can FT-IR provide?

- Identification of unknown organic and some inorganic materials, often mixtures and other microscopic.
- It can determine the quality or consistency of a sample.
- It can determine the amount of components in a mixture.

3.4.2 X-ray Diffraction

X-ray diffraction (XRD) is a versatile, non-destructive technique that reveals detailed information about the chemical composition and crystallographic structure of natural and manufactured materials. These techniques are based on observing the scattered intensity of an X-ray beam hitting a sample as a function of incident and scattered angle, polarization, and wavelength or energy.



Figure 3.7: X-ray Diffraction

X-ray diffraction has been most commonly used for routine characterization as well as for detailed structural elucidation. In order to obtain detailed structural information, knowledge of X-ray diffraction intensities is also essential, the intensities being related to the structure factor. Figure 3.7 shows XRD machine set up.

3.4.3 Wide angle X-ray diffraction

Wide angle X-ray Diffraction (WAXD) is a widely used instrument to identify crystalline structure of polymers. Their configurational determination of polymeric formation is highly dependent on time and data point. Diffracted angle of X-ray from surface can be defined by Bragg's Law (Figure 3.8),

$$n\lambda = 2d\sin\theta$$

where n is the order of a reflection, λ is the wavelength of X-ray, d is the distance between parallel lattice planes, and θ is the angle between the incident beam and a lattice plane.

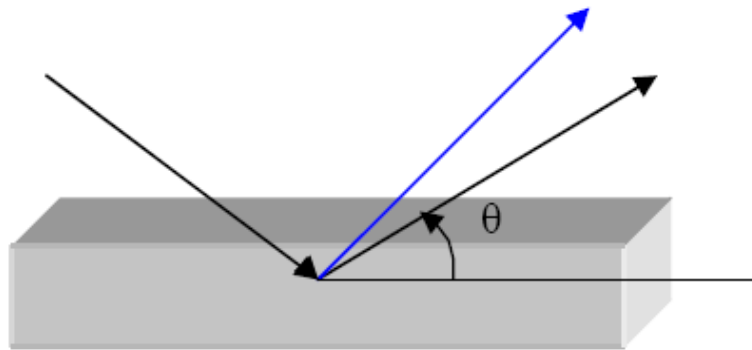


Figure 3.8: Principles of X-ray diffraction spectroscopy

Result can be measured by value of intensity or count and it can be possible to determine crystallite size and size distribution.

3.4.4 Scanning Electron Microscope (SEM)

The SEM is a microscope that uses electrons instead of light to form an image. SEM shows very detailed 3-D images at much higher magnifications than is possible with a light microscope. The SEM has a large depth of field, which allows more of a specimen to be in focus at one time.



Figure 3.9: Scanning Electron Microscope

How does a SEM work?

The SEM is an instrument that produces a largely magnified image by using electrons instead of light to form an image. A beam of electrons is produced at the top of the microscope by an electron gun (shown in fig 3.10). The electron beam follows a vertical path through the microscope, which is held within a vacuum. The beam travels through electromagnetic fields and lenses, which focus the beam down toward the sample. Once the beam hits the sample, electrons and X-rays are ejected from the sample (Shown in fig. 3.11).

Detectors collect these X-rays, **backscattered electrons**, and secondary electrons and convert them into a signal that is sent to a screen similar to a television screen. This produces the final image. Back-scattered electrons (BSE) are beam electrons that are reflected from the sample by elastic scattering.

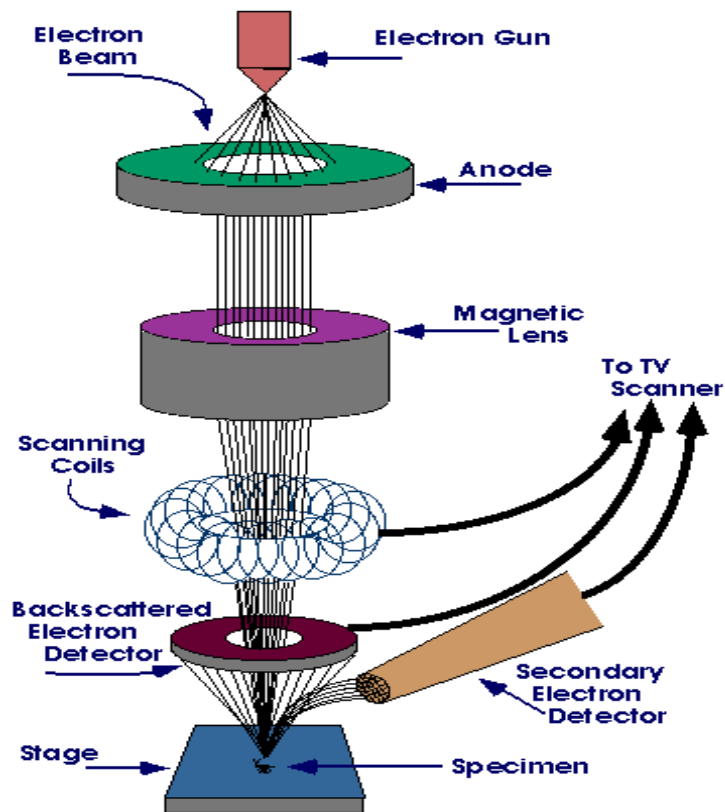


Figure 3.10: Working of SEM

BSE are often used in analytical SEM along with the spectra made from the characteristic X-rays. Because the intensity of the BSE signal is strongly related to the atomic number (Z) of the specimen, BSE images can provide information about the distribution of different elements in the sample.

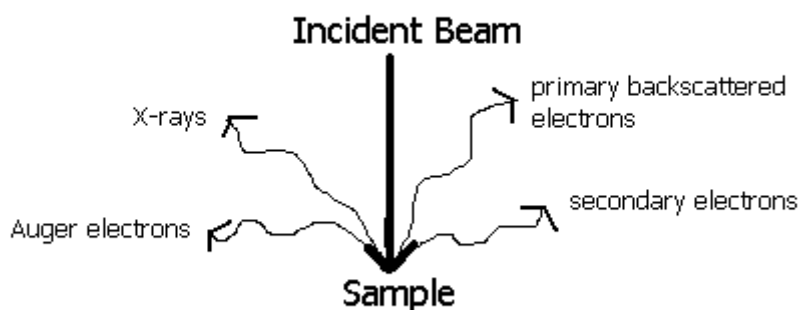


Figure 3.11: Interaction of incident beam with sample

3.4.5 Dielectric measurements

The dielectric measurements were carried out using a programmable automatic RCL meter (FLUKE PM 6306) in the frequency range 50Hz to 1MHz (fig 3.12) for thin films. The real and imaginary parts of the complex dielectric permittivity have been studied in detailed at different temperatures. The dielectric properties of the PVDF composites were taken at off voltages.



Figure 3.12: LCR Meter

In the case of polymeric medium, dielectric spectroscopy is a powerful technique that is capable of probing the molecular motion and the electric properties. The dielectric constant or relative permittivity of a material is the ratio of the dielectric constant of the material (ϵ) to that of vacuum (ϵ_0). The capacitance measures the extent to which charge can be stored.

$$\epsilon_r = \epsilon/\epsilon_0$$

Where ϵ_r is the relative permittivity of material.

A capacitor is formed when a non-conducting media, called the dielectric, separates two conducting plates. The value of the capacitance depends on the size of the plates, the distance between the plates and the properties of the dielectric.

The capacitance relationship is:

$$C = \frac{\epsilon_0 \epsilon_r A}{d}$$

With,

C = the capacitance

ϵ_0 = electrical permittivity

ϵ_r = relative electrical permittivity (dielectric constant)

A = surface of one plate

d = distances between two plates

The dielectric constant of material depends on the materials polarization, the higher the polarizability of molecule, higher the dielectric constant.

This chapter summarize the results which we obtained from the Fourier Transform Infrared Spectroscopy (FTIR), X-ray diffraction (XRD), Scanning Electron Microscope (SEM) and dielectric characterization to understand their chemical, structural, surface morphological and dielectric behaviour of pure PVDF film, PZT dispersed and ZnO nanoparticle dispersed PVDF film.

4.1 Chemical Analysis

Figure 4.1(a) represents the IR spectra (ranges from 4000 to 400 cm^{-1}) of PVDF film (5:5wt% THF/DMF) (a) as pure (b) Annealed at 90°C for 5hrs. The IR spectra of pure PVDF film exhibit peaks at 609.4 cm^{-1} corresponds to α -phase of PVDF while the peaks at 460.4, 842.0, 892.6 cm^{-1} represent the β -phase. The peak at 842 assigned to CF_2 asymmetric stretching vibrational mode. After annealing (90°C for 5h) we observed peaks at 463.7, 846, 892.6 cm^{-1} corresponding to β -phase while the peak at 481.7 represents the α -phase. So it cannot be concluded that annealing enhance the β -phase character. Some additional peaks observed in Pure and annealed films at 1075 cm^{-1} corresponds to the fluoro alkane.

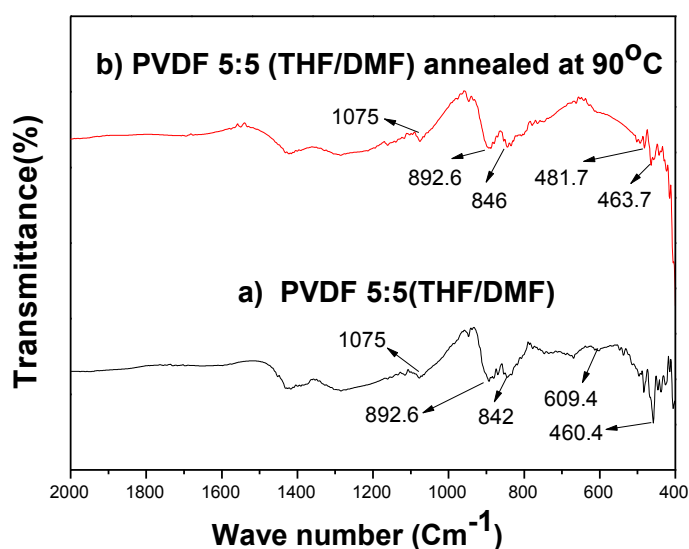


Figure 4.1(a): FTIR spectra of PVDF films cast with mass ratio of 5:5 (THF/DMF): a) as synthesised; b) Annealed at 90°C for 5hrs.

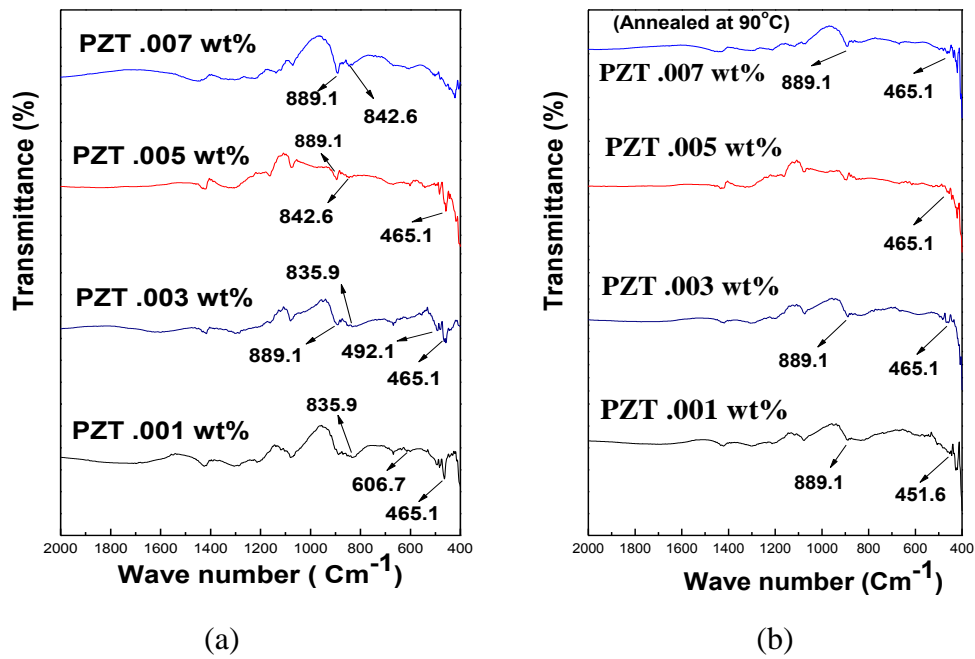


Figure 4.1(b): FTIR spectra of PVDF-PZT composite films at different concentration (.001, .003, .005, .007): a) as synthesized; b) Annealed at 90°C for 5hrs.

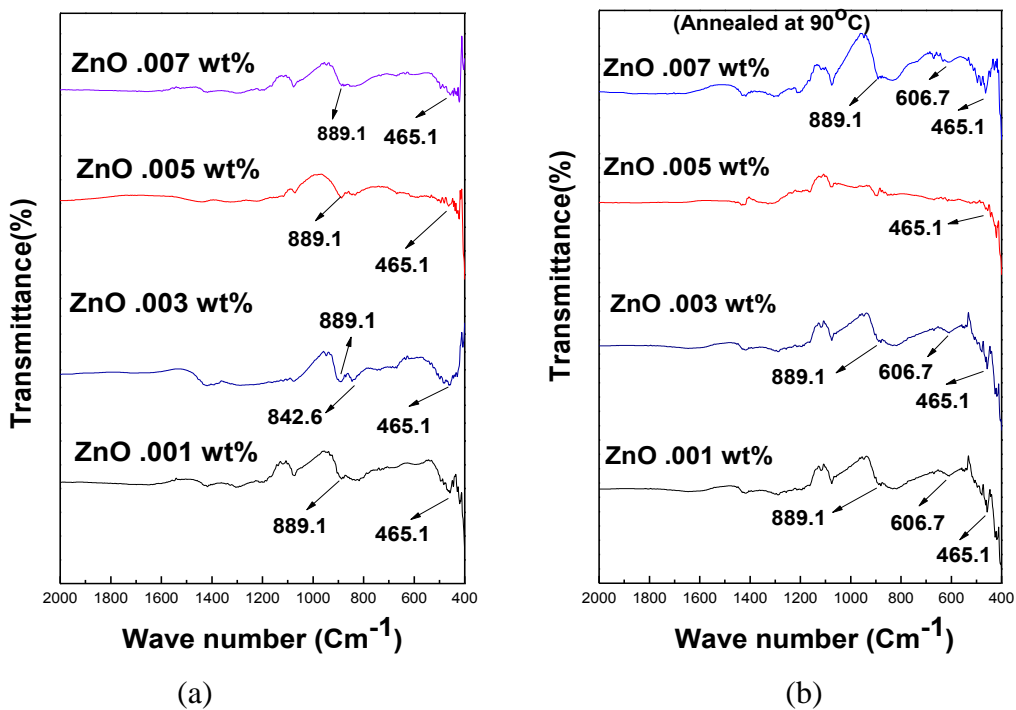


Figure 4.1 (c): FTIR spectra of PVDF-ZnO composite films at different concentration (.001, .003, .005, .007): a) as synthesized; b) Annealed at 90°C for 5hrs.

Figure 4.1(b) shows the FTIR spectra of PVDF-PZT composite film. The peaks at 606.7, 492.1 cm^{-1} corresponds to α -phase while peaks at 465.1, 842.6 and 889.1 cm^{-1} correspond to β -phase. We observed that as the concentration of PZT is increased, β -phase becomes dominant. After annealing we observed peak at 465.1, 851.6 and 889.1 indicating the presence of β -phase. So no effect of annealing has been observed.

Similarly the interaction between the ZnO nanoparticles in the PVDF matrix was observed from the infrared spectra shown in fig. 4.1(c). Observed peaks at 465.1, 842.5, 889.8 cm^{-1} indicate the presence of β -phase. No additional peak of ZnO has been found indicating the ZnO nanoparticles are homogeneously incorporated in the PVDF matrix.

4.2. Structural analysis

Wide angle X-ray diffraction (WAXD) was used to identify the crystalline phase of pure, PZT and ZnO nanoparticle dispersed PVDF composite films. Figure 4.2(a) shows the XRD pattern of (a) pure film and (b) film heated at 90°C. We observed well defined peaks at $2\theta=20.7^\circ$ corresponds to (200) plane for both pure and annealed sample indicate the presence of β -phase of PVDF. Diffraction peak at $2\theta=27.2^\circ$ also observed in case of Pure PVDF (without annealing) indicate the presence of α -phase. No significant effects of annealing have been observed.

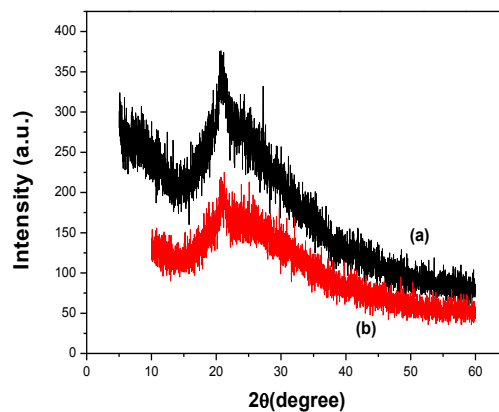


Figure 4.2 (a):X-ray diffraction pattern of PVDF film (a) without annealing (b) Annealed at 90°C

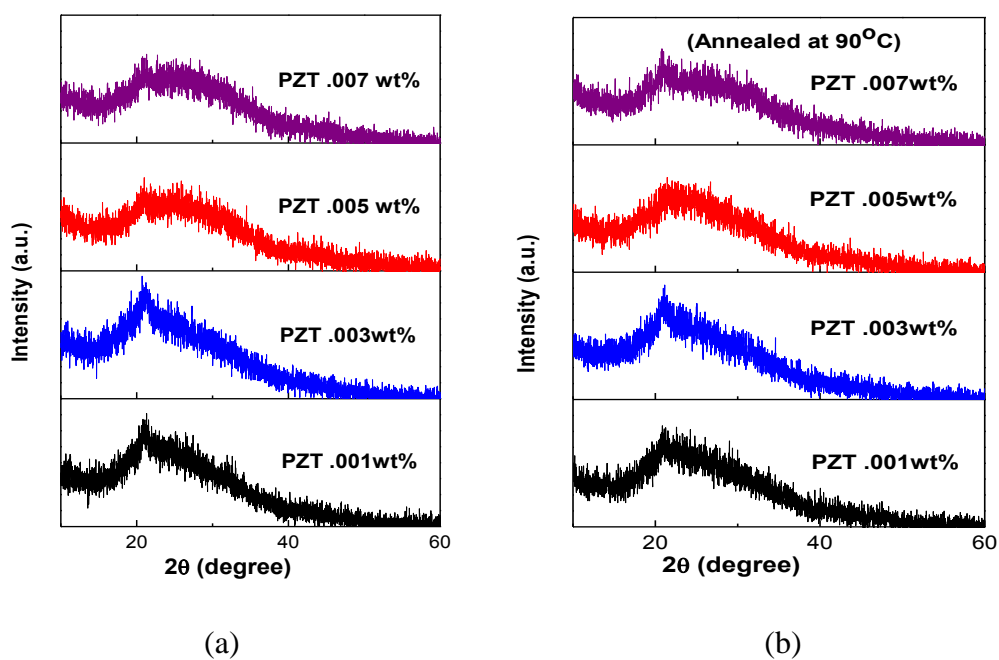


Figure 4.2 (b): X-ray diffraction pattern of PVDF/PZT composite film at varying concentration of PZT (.001, .003, .005, .007wt %) (a) Without annealing (b) Annealed at 90°C for 5hrs.

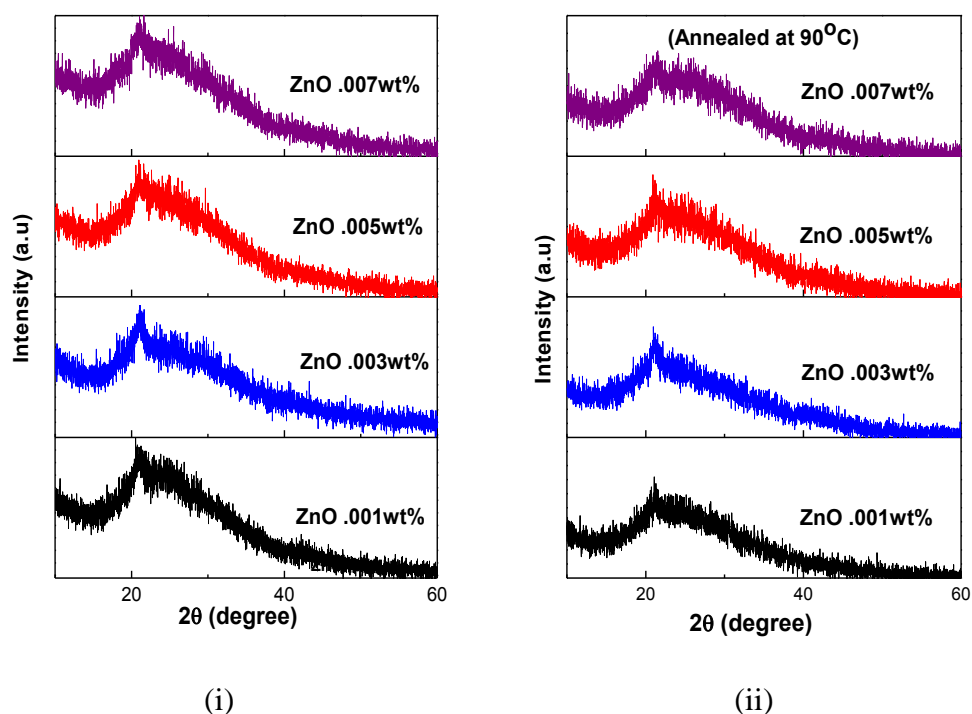


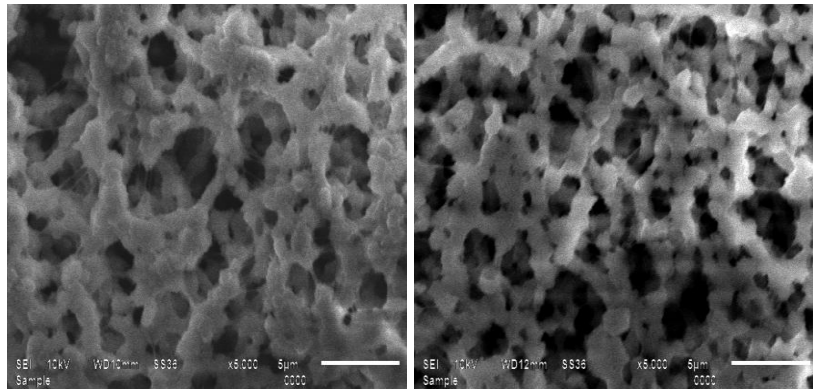
Figure 4.2 (c): X-ray diffraction pattern of PVDF/ZnO composite films at varying concentration of ZnO nanoparticle (.001, .003, .005, .007 wt %) (i) Without annealing (ii) Annealed at 90°C for 5hrs.

X-ray pattern of various concentration of PZT dispersed PVDF films are shown in fig. 4.2(b). The observed spectra indicate the presence of semicrystalline structure. Well defined peak formed at $2\theta=20.7^\circ$ at all concentration of PZT in without annealing film indicates the presence of β -phase. As the concentration of PZT increased the peak get broaden. We also made an attempt to study the effect of annealing on PZT dispersed PVDF film at a temperature (90°C for 5hrs). In annealed film we also observed peak at $2\theta=20.7^\circ$ indicates the presence of β -phase of PVDF refer to the (200) plane. From above results it is quite obvious to say that addition of PZT does not affect the structure of PVDF.

XRD patterns of ZnO nanoparticle dispersed PVDF films are shown in fig. 4.2(c), we observed peak at $2\theta=20.7^\circ$ indicative of β -phase of PVDF consistently for all concentration of ZnO dispersed in PVDF. In case of annealed sample (at 90°C) we observed peak at $2\theta=20.7^\circ$ for all sample attributed to the β -phase.

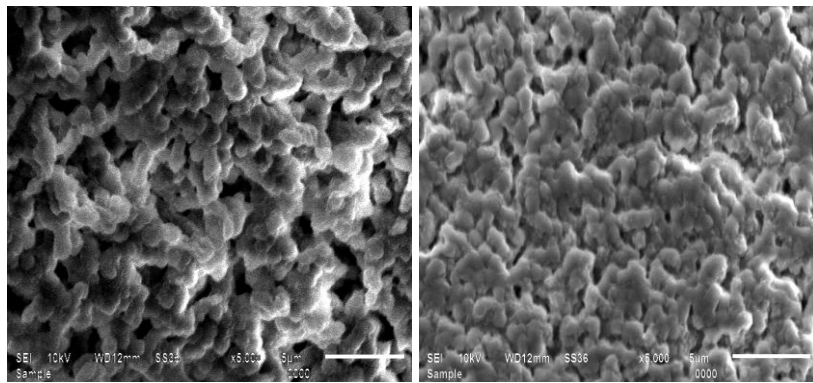
4.3 Morphological analysis of pure and nanoparticle dispersed PVDF composite films

SEM micrographs of pure, PZT and ZnO nanoparticle dispersed PVDF at different concentrations (.001, .003, .005, .007wt %) are shown in fig 4.3(a) (i-v) and 4.3(b) (i-v) at 5000X magnification. SEM image shows the cellular nature of pure PVDF. We observed that in all cases size of pores is reduced by filling of PZT and ZnO nanoparticle. From SEM image of PZT dispersed PVDF composite film (fig.4.3(a) (i-v))we observed that as the concentration of PZT increased the size of the pores is reduced while at very high concentration (.007 wt%) we observed increment in the size of pores. The uniformity of ZnO nanoparticle dispersion is clear from fig.4.3 (b) (ii-v). It was also found that the fine spherulites were arranged in well defined fashion in all cases. Well defined network of spherulites may give rise to the dielectric constant in the composite systems.



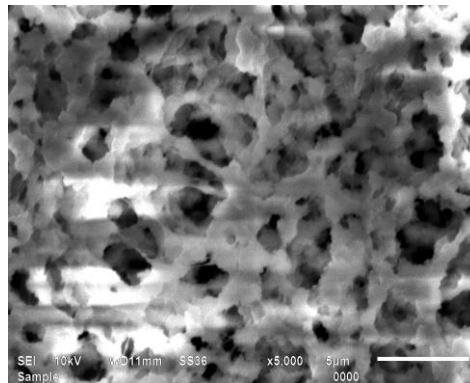
(i) Pure

(ii) PZT .001wt%



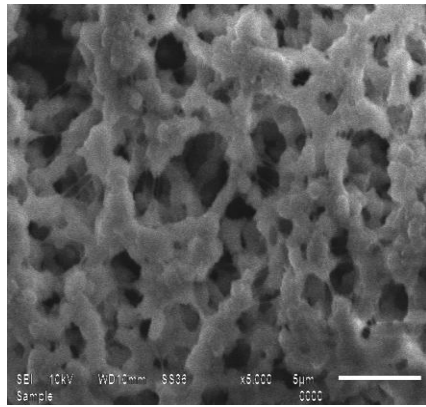
(iii) PZT .003 wt%

(iv) PZT.005wt%

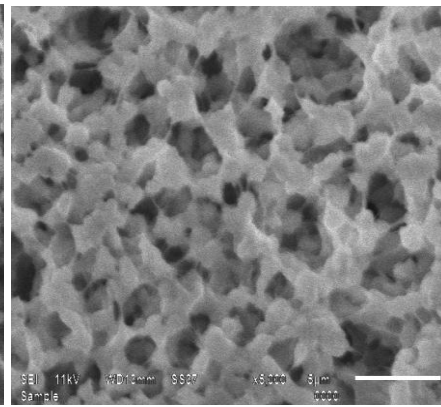


(v) PZT .007

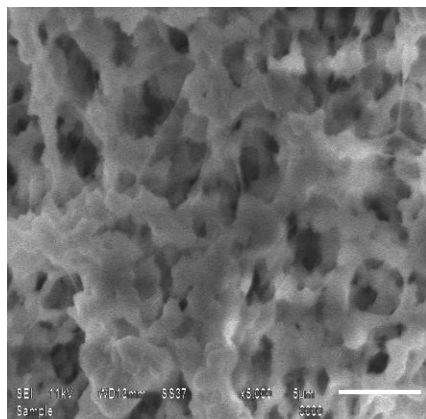
Figure4.3 (a): SEM micrograph of pure and PZT dispersed PVDF films at 5000X.



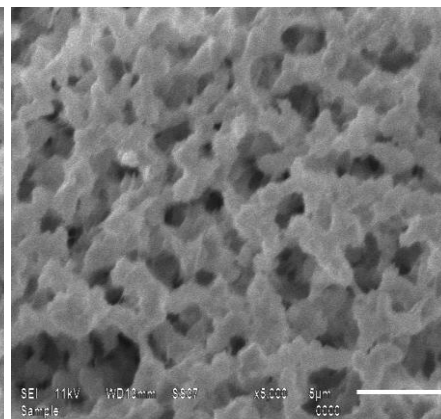
(i) Pure PVDF



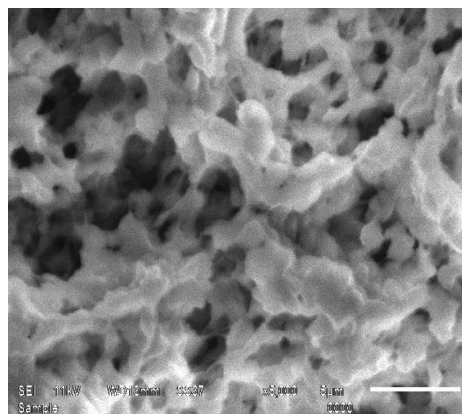
(ii) ZnO .001wt%



(iii) ZnO .003 wt%



(iv) ZnO .005wt%



(v) ZnO .007wt%

Figure4.3 (b): SEM micrograph of pure and ZnO nanoparticle dispersed PVDF films at 5000X.

4.4 Dielectric spectroscopy

The temperature and frequency dependent dielectric behaviour of thin film of PZT and ZnO dispersed PVDF in the frequency range 50Hz to 1MHz and temperature range 30°C to 180°C has been studied.

4.4.1 Dielectric study of PVDF-PZT composite film

4.4.1.1 Frequency and temperature dependence of relative permittivity (ϵ')

The variation in relative permittivity (ϵ') as function of frequency for pure, PZT dispersed PVDF samples are shown in figure 4.4(a). We observed that very low concentration (.001 wt %) gives rise to relative permittivity and attain maxima (45) in the lower frequency region. However rest of the concentration displayed the permittivity around pure PVDF. At higher frequency no significant dispersion has been observed.

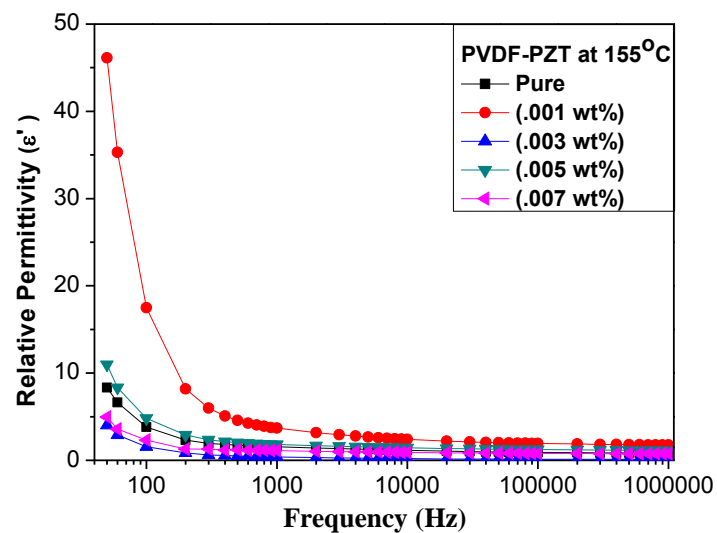


Figure 4.4(a): Variation of relative permittivity with frequency at different concentrations of PVDF/PZT at 155°C.

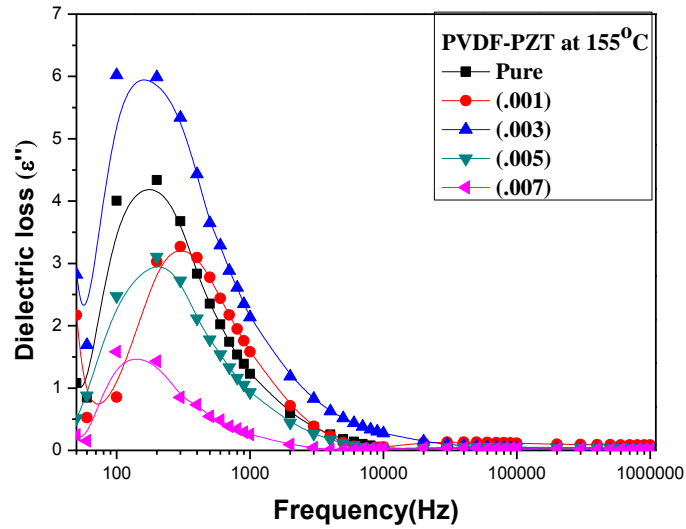


Figure 4.4 (b): Variation of dielectric loss with frequency at different concentrations of PVDF/PZT at 155°C.

The variation of dielectric loss of pure PVDF and PZT dispersed films are shown in figure 4.4(b). We observed that at low frequency dielectric loss slightly increases upto concentration (.003 gm). The gradual decrease in the loss factor has been observed with further increasing concentration. At higher frequencies there was no significant variation in dielectric loss has been observed.

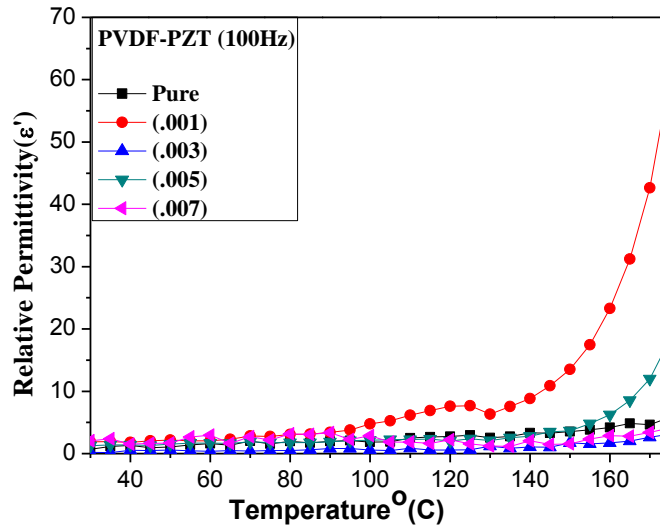


Figure 4.4(c): Variation of relative permittivity with temperature at different concentrations of PVDF/PZT at 100 Hz.

Figure 4.4(c) shows the variation in relative permittivity as a function of temperature at 100 Hz. At low frequency (100Hz) we found increase in dielectric constant as concentration of

PZT increases. At higher temperature, abrupt variation in relative permittivity was observed in the temperature region of 160°C to 175°C.

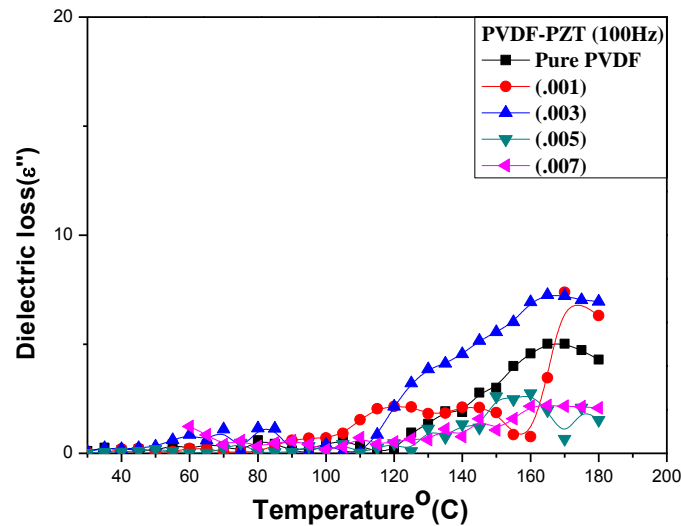


Figure 4.4(d): Variation of dielectric loss with temperature at different concentrations of PZT in PVDF at 100 Hz.

Figure 4.4(d) (ii) shows the variation of dielectric loss with temperature at different concentration of PZT at 100Hz. We observed that the loss is maximum at .001 and .003 wt% concentration, though, the magnitude of loss factor is small.

Such increase in the PZT dispersed sample at lower concentration attributed to the better incorporation of PZT particle in the PVDF matrix and the contribution of the coupled dipole moment of PVDF and PZT, which spontaneously enhance the permittivity at lower concentration.

4.4.2 Dielectric study of PVDF-ZnO composite film

4.4.2.1 Frequency and temperature dependent relative permittivity (ϵ')

The variation in relative permittivity as function of frequency for pure, ZnO nanoparticle dispersed PVDF samples are shown in figure 4.4(e). We observed that at lower concentrations of ZnO nanoparticles, the relative permittivity of PVDF-ZnO composite was not much influenced. As the amount of doping increased to .007 wt%, we found increase in the value of relative permittivity at low frequency region. The dielectric constant of a material generally comprises four types of contributions, namely, ionic, electronic orientational and space charge polarisations.

All these may be active at low frequencies and the nature of variations of dielectric constant with frequency indicates the type of contributions that are present in them. Udupa et al. [46] have reported that the large value of dielectric constant at low frequency is due to the presence of space charge. PVDF is a polar polymer. When the frequency is increased the dipoles do not have enough time to align before the field changes the direction and the dielectric permittivity and dielectric loss decreases.

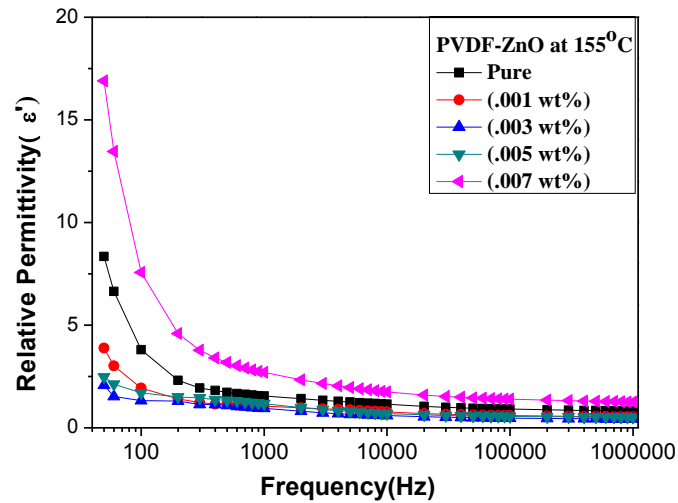


Figure 4.4(e): Variation of relative permittivity with frequency at different concentrations of ZnO nanoparticle in PVDF

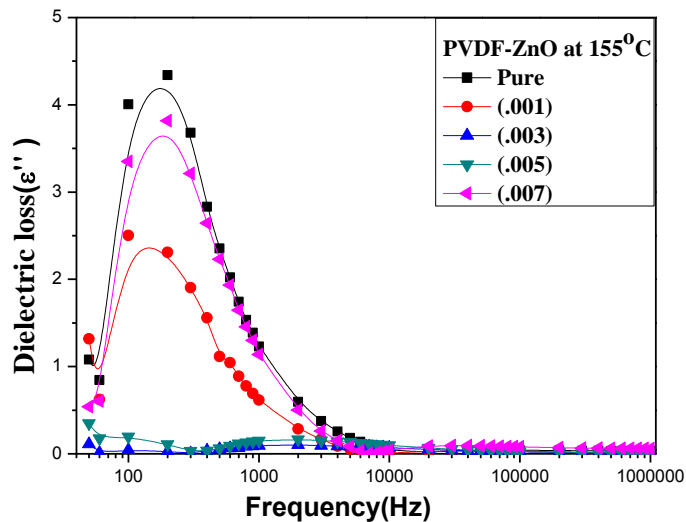


Figure 4.4(f): Variation of dielectric loss with frequency at different concentrations of ZnO nanoparticle in PVDF at 155°C.

The variation of dielectric loss in PVDF-ZnO composite with frequency at different concentration of ZnO nano particles at 155°C are shown in figure 4.4(f). We observed that as

the frequency was increased the loss factor was decreased. Dielectric loss of PVDF-ZnO composite is lower than pure PVDF.

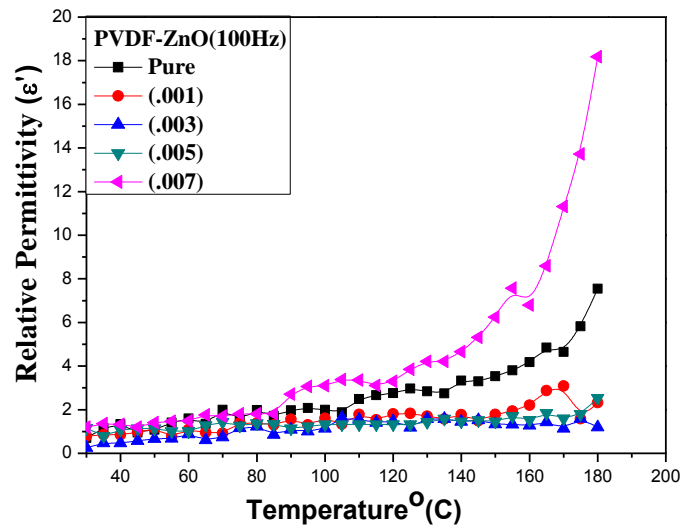


Figure 4.4(g): Variation of relative permittivity Vs temperature at different concentrations of ZnO nanoparticle in PVDF at 100Hz.

Figure 4.4(g) shows the variation of relative permittivity at 100 Hz as a function of temperature for different concentration of ZnO nanoparticle dispersed in PVDF. We observed that at low temperature the relative permittivity was not much influenced. As the temperature increased relative permittivity increases for higher concentration of ZnO with temperature.

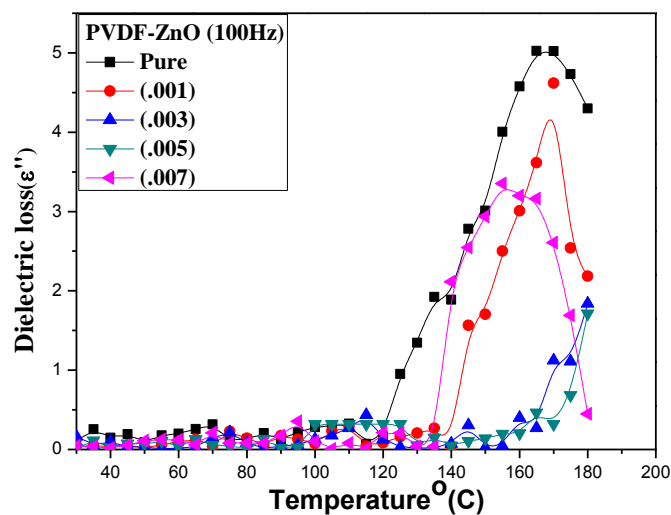


Figure4.4 (h): Variation of dielectric loss with temperature at different concentrations of ZnO nanoparticle in PVDF at 100Hz.

Figure 4.4(h) shows the variation of dielectric loss at 100 Hz as a function of temperature for different concentration of ZnO nanoparticle dispersed in PVDF. We observed there was a sudden increase in the dielectric loss at transition temperature and it was become maximum near its melting temperature after that it start to decrease.

Table 4.1 Comparison of relative permittivity of composite films samples at different concentration

Concentration (wt %)	Pure	.001	.003	.005	.007
Relative Permittivity of PZT-PVDF composite film	8.3	45	4	11	5
Relative Permittivity of ZnO-PVDF composite film	8.3	4	2	2.5	17

4.5 Conductivity measurement

The conductivity of PZT and ZnO nanoparticle dispersed PVDF composite films was calculated and plotted as a function of temperature and frequency.

4.5.1 PVDF-PZT composite film

Figure 4.5(a) shows the variation of conductivity with frequency. We observed that the effect of frequency highlights only in the high frequency range. Whereas for higher concentration of PZT (.007 wt %) conductivity in high frequency region was not much influenced. However at low frequency region conductivity is almost constant.

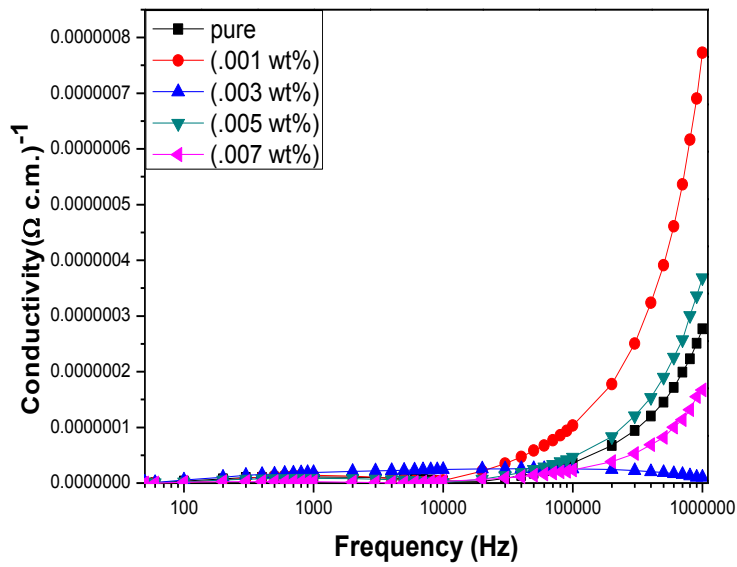


Figure 4.5 (a): Conductivity measurement of PVDF-PZT system with frequency at 155°C.

From fig 4.5(b) we found that the conductivity increase with increasing temperature. The increment in temperature provides an increase in free volume and segmental mobility. These two entities then permits free charges to hop from one site to another thus increase conductivity. [47]

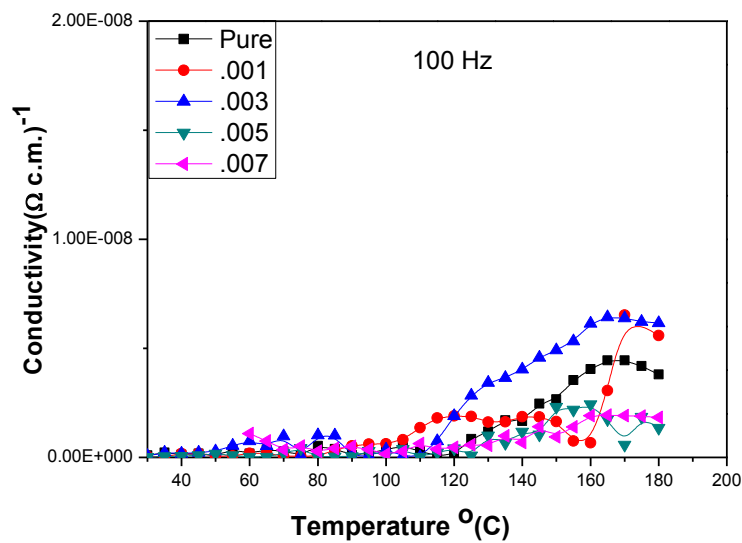


Figure 4.5 (b): Conductivity measurement of PVDF-PZT system with temperature at 100 Hz.

4.5.2 PVDF-ZnO composite film

From fig. 4.5(c) it is clear that the conductivity shows a small change in the low frequency range while increases at higher frequency for higher concentration of ZnO content.

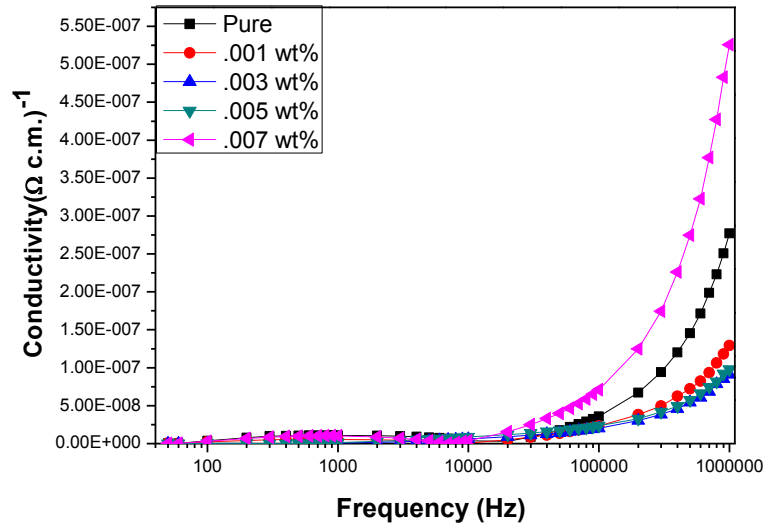


Figure 4.5(c): Conductivity measurement of PVDF-ZnO system with frequency at 155°C.

Figure 4.5(d) shows the variation of conductivity with increasing temperature and ZnO concentration. In this case conductivity does not show any significant change as the ZnO-PVDF composite films shows decrease in magnitude of conductance than that of pure PVDF. The sharp increase of conductivity between 160°C to 170°C can be attributed to large heat energy absorbed by the samples and thus induce mobility of electrons [47].

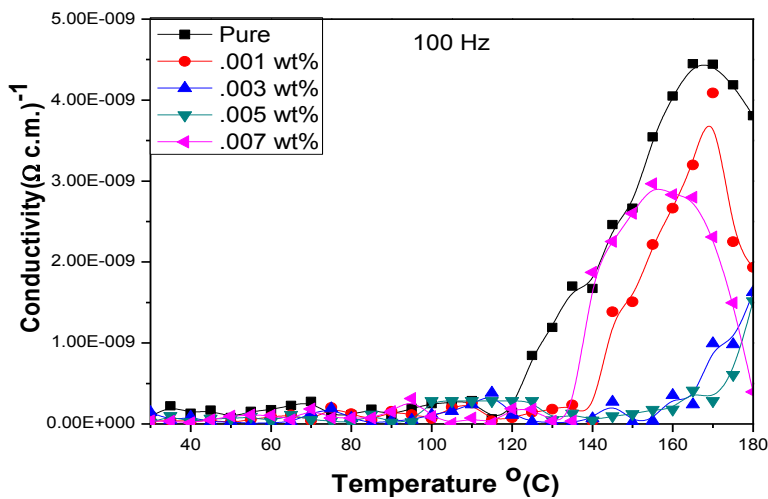


Figure 4.5(d): Conductivity measurement of PVDF-ZnO system with temperature

Table4.2: Comparison of conductivity of composite films samples at different concentration

Concentration (wt%)	Pure	.001	.003	.005	.007
Conductivity of PZT- PVDF composite film	2.7×10^{-7}	7.7×10^{-7}	1.2×10^{-8}	3.6×10^{-7}	1.7×10^{-7}
Conductivity of ZnO- PVDF composite film	2.7×10^{-7}	1.3×10^{-7}	9×10^{-8}	9.8×10^{-8}	5.2×10^{-7}

CONCLUSION

CONCLUSION

- PVDF polymer and their properties, phase conformation, and analytical methods were reviewed at the beginning of this thesis. The thin films of pure PVDF and nanomaterial dispersed PVDF with mass ratio of 5:5 (THF/DMF) were fabricated by using spin coating.
- X-ray diffraction and FTIR analysis confirmed the formation of pure well crystalline β -phase. From chemical analysis we observed that as the concentration of PZT content increased, β -phase become dominant. Also ZnO dispersed PVDF film indicate the presence of β -phase. Further formation of well defined β -phase has been confirmed from XRD analysis. No significant effect of annealing has been observed.
- Morphological investigations suggesting that the nanomaterials are uniformly dispersed in the PVDF matrix.
- From dielectric studies we found that the permittivity decreases with frequency due to orientational polarisation and increases with temperature. The relative permittivity of PZT dispersed composite film attains maxima 46 at very low concentration (.001gm) and then decline at higher concentration. Whereas the relative permittivity of ZnO dispersed nanocomposites film attain a maximum value at (17) at higher concentration (.007 gm) and having less value at lower concentration. Loss factor decreases with increasing frequency and concentration of PZT and ZnO nanoparticles.
- The conductivity calculated for PZT-PVDF composite films shows the increment with the increase in temperature and PZT content. While in case of ZnO dispersed PVDF composite films conductivity was not much influenced. As the temperature increases, the polymer can expand easily and produce free volume.

REFERENCES

- [1] Glushanin, S.; Topolov, V. Y.; Krivoruchko, A. V.; "Features of piezoelectric properties of 0-3 PbTiO₃-type ceramic/polymer composites", *Materials Chemistry and Physics* 97 (2-3), 357-364, (2006).
- [2] Hine, P.; Broome, V.; Ward, I.; "The incorporation of carbon nanofibres to enhance the properties of self reinforced, single polymer composites", *Polymer* 46 (24), 10936-10944, (2005).
- [3] Cioffi, N.; Torsi, L.; Ditaranto, N.; Tantillo, G.; Ghibelli, L.; Sabbatini, L.; Bleve-Zacheo, T.; D'Alessio, M.; Zambonin, P. G.; Traversa, E.; "Copper nanoparticle/polymer composites with antifungal and bacteriostatic properties", *Chemistry of Materials* 17 (21), 5255-5262, (2005).
- [4] Pelaiz-Barranco, A.; Marin-Franch, P.; "Piezo-, pyro-, ferro-, and dielectric properties of ceramic/polymer composites obtained from two modifications of lead titanate", *Journal of Applied Physics* 97 (3) (2005).
- [5] Elashmawi, I.S.; "Effect of NaCl filler on ferroelectric phase and polaron configurations of PVDF films", *Cryst. Res. Technol.* 42, 389-393, (2007).
- [6] V. L. Strashilov, "Efficiency of Poly (Vinylidene Fluoride) Thin Films for Excitation of Surface Acoustic Waves," *Journal of Applied Physics* 88, 3582–3586 (2000).
- [7] N. Fujitsuka, J. Sakata, Y. Miyachi, K. Mizuno, K. Ohtsuka, Y. Taga, and O. Tabata, "Monolithic Pyroelectric Infrared Image Sensor Using PVDF Thin Film," *Sensors and Actuator A* **66**, 237–243 (1998).
- [8] Arunkumar Lagashetty and A Venkataraman,"Polymer Nanocomposites", Article in resonance June (2005).
- [9] T.Tanaka, G. C. Montanari and R. Mulhaupt, *IEEE Trans. Dielectr. Electr. Insul.* 11, pp.763-783, 2004.
- [10] T. J. Lewis, *IEEE Trans. Dielectr. Electr. Insul.* 11, pp.739-753, 2004.
- [11] Tanaka T, Kozaka M, Fuse N, Ohki Y. Proposal of a multi-core model for polymer nanocomposite dielectrics. *IEEE Trans Dielectr Electr Insul.* 2005; 12:669–81.
- [12] Nalwa, H. S., "Ferroelectric Polymers": Chemistry, Physics and Applications. Marcel Dekker, Inc., New York: 1995.
- [13] T.R. Jow and P.J. Cygan, *J. Appl. Phys.* 73, 5147 (1993).
- [14] N. Murayama, *J. Polymer. Sci.* 13, 929 (1975).

- [15] Youn Jung Park, Hee June Jeong, Jiyoun Chang, Seok Ju Kang, and Cheolmin Park; “Recent development in polymer ferroelectric field effect transistor memory”; *Journal of semiconductor technology and science*, vol.8, no.1, March, 2008.
- [16] Q X Chen, PA Payne; “Industrial applications of piezoelectric polymer transducers”; *Meas. Sci. Technol.* 6 (1995) 249-267. UK.
- [17] Stroyan, J.; “Processing and Characterization of PVDF, PVDF-TrFE, and PVDFTTrFE-PZT Composites. Master Thesis”: Washington State University, Pullman, Washington, 2004.
- [18] Nalwa, H. S., “Ferroelectric Polymers: Chemistry, Physics and Applications”: Marcel Dekker, Inc., New York: 1995.
- [19] Lovinger, A., “Poly (viylidene fluoride), in Developments in Crystalline Polymers-1”: Applied Science Publishers, London: 1982.
- [20] M. G. Broadhurst and G. T. Davis; “Piezo- and Pyroelectric Properties”.
- [21] Jordan, T. L. and Z. Ounaies. “Piezoelectric Ceramics Characterization”. *Encyclopedia of Smart Materials*. Wiley Interscience.
- [22] Taylor, G.W., Gagnepain, J.J., Meeker, T.R., Nakamura, T., and Shuvalov, L.A., 1985, *Piezoelectricity*, Gordon and Breach Science Publishers, New York.
- [23] Ku, Chen C. and Raimond Liepins.; “Electrical Properties of Polymers Chemical Principles”: New York: Hanser Publishers.
- [24] Stroyan, J.; “Processing and Characterization of PVDF, PVDF-TrFE, and PVDFTTrFE-PZT Composites. Master Thesis”: Washington State University, Pullman, Washington, 2004.
- [25] M.M.D. Ramos, H.M.G. Correia, and S. Lanceros-Mendez. ; “Atomistic modelling of processes involved in poling of PVDF”: *Comp. Mater. Sci.*, 33:230–236, 2005
- [26] M.M. Perlman and M. Canada. Patent; “Method to double the piezo-and pyroelectric constant of polyvinylidene fluoride (pvdf) film”: October 1993.
- [27] T.R. Dargaville, M.C. Celina, J.M. Elliott, P.M. Chaplya, G.D. Jones, D.M. Mowery, R.A. Assink, R.L. Clough, and J.W. Martin.; “Characterization, performance and optimization of PVDF as a piezoelectric film for advanced space mirror concepts”: Technical Report SAND2005-6846, Sandia National Laboratories, 2005.
- [28] Y. Zhang, K. Suenaga, C. Collies, S. Iijima, *Science* 281 (1998) 973.
- [29] L. Vayssieres, K. Keis, A. Hagfeldt, S.-E. Lindquist, *Chem. Mater.* 13 (2001) 4395.
- [30] Z. W. Pan, Z. R. Dai, Z. L. Wang, *Science* 292 (2001) 1947.
- [31] Lovinger, A.J., 1983; “Ferroelectric polymers,” : *Science*, **220**(4602), pp. 1115-1121.
- [32] Wang, T.T., Herbert, J.M., and Glass, A.M., 1988, “The Applications of Ferroelectric Polymer”, Blackie, New York.

- [33] Hasegawa, R., Takahashi, Y., Chatani, Y., and Tadakoro, H., 1972, "Crystal structures of three crystalline forms of poly (vinylidene fluoride)," *Polym. J.*, **2**, pp. 600-610.
- [34] Wenzhong Ma E Jun Zhang E Xiaolin Wang; "Formation of PVDF crystalline phases from THF/DMF mixed solvent": *Journal of Material Science*, 43, 398-401, (2008).
- [35] Kawai, H., 1969; "The piezoelectricity of poly (vinylidene fluoride)": *Japan J. App. Phys.*, **8**, pp. 975-976.
- [36] Bergman, J.G., McFee, J.H., and Crane, G.R., 1971; "Pyroelectricity and Optical second harmonic generation in polyvinylidene fluoride films": *Appl. Phys. Lett.*, **18**, pp. 203-203.
- [37] Nakamura, K., and Wada, Y., 1971; "Piezoelectricity, pyroelectricity, and the electrostriction constant of poly (vinylidene fluoride)," *J. Polym. Sci.*, **A-29**, pp. 161-173.
- [38] Barsky M. F., Lindner D. K., and Claus R.O., 1989; "Robot gripper control system using PVDF piezoelectric sensors,": *IEEE Transactions on Ultrasonics, Ferroelectrics, and Frequency Control*, **36**(1), pp. 129-134.
- [39] Ajayan PM, Stephan O, Colliex C, Trauth D.: "Aligned Carbon Nanotube Arrays Formed by Cutting a Polymer Resin-Nanotube Composite": *Science*; 265: 1212-1214, (1994).
- [40] Namrata Shukla, Archana Shukla, Awalendra K. Thakur and R. N. P. Chaudhary; "Low Temperature Ferroelectric Behaviour of PVDF Based Composites": *Indian Journal of Engineering & Materials Science*, 15(2), 126-132 (2008).
- [41] Yi and Liang; "A pvdf-based deformation and motion sensor: modelling and experiments": *IEEE sensors journal*, vol. 8, no. 4, April 2008.
- [42] D.R. Dillon et al.: "On the structure and morphology of polyvinylidene fluoride–nanoclay nanocomposites in Science Direct"; 47 (2006) 1678–1688.
- [43] Gaur M.S., Indolia A.P; "Thermally stimulated dielectric properties of polyvinylidene fluoride-zinc oxide nanocomposites"; *J Therm Anal Calorim* (2011) 103:977-985.
- [44] Zhang De-Qing, Wang Wa-Wei, Yuan Jie, Zhao Quan-Liang, Wang Zhi-Ying, Cao Mao-Sheng; "Structural and Electrical Properties of PZT/PVDF Piezoelectric Nanocomposites Prepared by Cold-Press and Hot-Press Routes"; *CHIN.PHYS.LETT.*; Vol. 25, No. 12 (2008) 4410.
- [45] Haixiong Tang, Yirong Lin, Clark Andrews and Henry A Sodano; "Nanocomposites with increased energy density through high aspect ratio PZT nanowires"; *IOP PUBLISHING; Nanotechnology* **22** (2011) 015702 (8pp).

- [46] K. Somasekhara Udupa, P. Mohan Rao, S. Aithal, A.P. Bhat, and D.K. Avasthi, “Effect of heavy-ion irradiation on dielectric constant and electrical conductivity of doped and undoped nonlinear substance”, *Bull. Mater. Sci.* 20 (1997), pp. 1069–1077.
- [47] Tominaga, Y., S. Asai, M. Sumita, S. Panero and B. Scrosati. 2005. “A novel composite polymer electrolyte: Effect of mesoporous SiO₂ on ionic conduction in poly (ethylene oxide)–LiCF₃SO₃ complex”. *Power Source*, 146: 402-406.